Characterizing Interactions of Thioflavin-T with Native Proteins Especially Bovine Serum Albumin

by

Caleb Matthew Stratton

April, 2017

Director of Thesis: Atta Ahmad (PhD)

Major Department: Biology

Abstract

Thioflavin T is a fluorescent probe used to monitor formation of cross β-sheet rich amyloid fibrils. Involvement of the amyloid fibrils is implicated in more than 50 human diseases, such as Alzheimer's, Parkinson's and Prion's. The proteins responsible for each of these diseases many as well as model proteins have been used to unravel the process involved in native protein to amyloid transformation, especially, for drug design but with little success thus far. Bovine serum albumin (BSA), predominantly α-helical in constitution, is one such protein that has been observed to transform to β-sheet rich amyloid. For our thesis project, we set on with these basic lines of evidence for ThT and BSA and devised a study outline. The study was divided into sub sections for better redressal compared to what was reported in literature viz., 1) Characterizing the steps involved in the transformation of BSA from native to amyloid state, 2) Develop methodology to gain information of as many steps as possible, 3) Identify the structural changes triggering BSA on pathway to fibrillation, 4) Computational comparison of the sites with chaperone binding sites and finally 5) if from point 4 we could observe chaperones interfering the aggregation process of BSA. During this thesis work, we observed an unexpected interaction of the reporter ThT molecule with the native BSA. We expanded this further and used a suite of

standard proteins and found that ThT has the unlikely affinity to bind to some of the proteins, which are predominantly helical in nature.

The present study thus details the aspects of interaction of ThT with BSA. Briefly, our Fluorescence data indicated a strong binding of ThT with BSA, ovalbumin and Alcohol Dehydrogenase. The binding was confirmed with ELISA type binding assays. Further, Circular dichroism showed ThT binding caused a minor structural disruption in the alpha helical content of the BSA which was supported by melting curves where BSA in the presence of ThT was 4 degrees less stable than in the absence of ThT. A control run of myoglobin exhibited no changes in the Tm studies with ThT. In addition, FTIR data exhibited marked changes in the BSA profiles in the presence and absence of ThT. Based on these data we ran the molecular docking simulation on ThT and BSA crystal structure and shortlisted two most predictable binding sites of ThT on BSA.

Characterizing Interactions of Thioflavin-T with Native Proteins Especially Bovine Serum Albumin

A thesis

Presented to

The faculty of the Department of Biology

East Carolina University

In Partial Fulfillment

of the Requirement of the Degree

Masters of Science in Biology

By

Caleb Matthew Stratton (B.Sc)

April 2017

Characterizing Interactions of Thioflavin-T with Native Proteins Especially Bovine Serum Albumin

By

Caleb Matthew Stratton

APPROVED BY:

DIRECTOR OF

THESIS: _____

Jean-Luc Scemama, Ph.D.

CO-DIRECTOR: _____

Atta Ahmad, Ph.D.

COMMITTEE MEMBER: _____

Paul Hager, Ph.D.

COMMITTEE MEMBER: _____

Ed Stellwag, Ph.D.

COMMITTEE MEMBER: _____

Cindy Putnam-Evans, Ph.D.

CHAIR OF THE DEPARTMENT

OF BIOLOGY: _____

Jeffrey McKinnon, Ph.D.

DEAN OF THE

GRADUATE SCHOOL: _____

Paul J. Gemperline, Ph.D.

Table of Contents

List of Tables ***Page***

List of figures ***Page***

List of Abbreviations

1. 5-FU- 5-fluorouracil
2. AA- Amino acids
3. AChE- Acetylcholinesterase
4. AD- Alzheimer's Disease
5. ALB- Serum albumin precursor
6. APACHE III- Acute Physiology and Chronic Health Evaluation
7. AZ- azacitidine
8. Aβ- Amyloid beta protein
9. BSA- Bovine Serum Albumin
10. BTA-1- 2-(4'-Methylaminophenyl) benzothiazole
11. CD- Circular dichroism
12. CFX- Cefixime
13. CMC- Critical micellar concentration
14. COP- colloid oncotic pressure
15. CY- cytarabine
16. Cy-3-G- Cyanidin-3-glucoside
17. DI- Deionized
18. DnaK OR Hsp70 - 70 kilodalton heat shock proteins
19. DTT- Dithiothreitol
20. EDTA- Ethylenediaminetetraacetic acid
21. ELISA- Enzyme-linked immunosorbent assay
22. EM- Electron microscopy

23. ESA- Equine serum albumin

24. F-Fast moving low pH transition

25. F-E- Equilibrium transition

26. FPLC- Fast protein liquid chromatography

27. FTIR- Fourier transform infrared spectroscopy

28. GEM- Gemcitabine Hydrochloride

29. HCl- Hydrochloric acid

30. HSA- Human Serum Albumin

31. IL-6- Interleukin 6

32. K_d- Disassociation constant

33. MA- Magniferin

34. MMR- Measles, Mumps and Rubella vaccine

35. MMRV- Measles, Mumps, Rubella, and Varicella vaccine

36. mRNA- Micro ribonucleic acid

37. MTX- Mitoxantrone

38. N-Native

39. B- Base, high pH transition

40. NO- Nitric oxide

41. NOT- Nortriptyline hydrochloride

42. PAGE- Polyacrylamide gel electrophoresis

43. PDB- Protein databank

44. PEG- Poly(ethylene glycol)

45. pH- Potential of hydrogen

46. PMSF- Phenylmethylsulfonyl fluoride

47. PMZ- Promazine hydrochloride

48. PSAM- Peptide self-assembly mimic

49. RNAse- Ribonuclease

50. RPM- Rotations per minute

51. RT- Room temperature

52. SD- Sulfadiazine

53. SDS- sodium dodecyl sulfate

54. SEC- Size exclusion chromatography

55. TEM- Transmission electron microscopy

56. ThT- Thioflavin T

57. TNF-a- Tumor necrosis factor alpha

Introduction

For this thesis, we have focused on exploring the interaction of ThT with standard proteins and especially BSA. ThT is mainly used for characterization of amyloid aggregation. We will start with the description of amyloid, followed by BSA and then ThT to cover the bases of this thesis project.

Amyloid: Proteins can aggregate in mainly two different forms i) unordered masses like precipitates and inclusion bodies and ii) ordered structures resulting in a characteristic final form. Amyloids are the ordered aggregates of proteins that are formed because of intermolecular β-sheet formation between different molecules attached side to side that appears like a fiber in the EM pictures (Cohen and Calkins, 1959). In each fiber, the individual proteins molecules are stacked so that their long axis lies perpendicular to the long axis of the fiber. This arrangement is also termed as cross β-sheet structure. Further the individual molecules may form a parallel or antiparallel β-sheet (Eanes and Glenner, 1968). The amyloid formation is interesting phenomenon and is observed by most proteins under right conditions including mostly helical proteins like myoglobin (Fändrich et al., 2001). This generality has therefore added to the intrigue of understanding amyloid. The transformation of protein irrespective of its initial native structure to a unique amyloid has fascinated protein biophysicists and folding experts for years. But the involvement of amyloid in human diseases especially Alzheimer's, Parkinson's, Prion's, Huntington's and other more than 50 types of human diseases hijacked the mere basic scientific fascination into an imperative applicative problem that needs immediate address and attention. The discovery of amyloid fibers being a part of the plaque in the postmortem Alzheimer's brain initiated the socio-medical interest in amyloid. The amino acid sequence of the constituents of this plaque laid further the founding stones of amyloid-protein diseases and connected these to

the larger biochemistry, cell biology, physiology ending at gene identification and location (Glenner and Wong, 1984). The gene linkage finally endowed the familial nature to these diseases (Kang et al., 1987). Unfortunately, these lines have not moved a long distance and in such scenario the protein biochemistry/biophysics involvement in these diseases attracts most of the focus. It was also observed a particular protein was involved in a particular disease for example, Aβ peptides and tau cause AD, synucleins are involved in Parkinson's, huntingtin in Huntington's and prion in mad cow disease. The species barrier and cross amyloid barrier has added to the mystery further but we cannot venture into those details at this point. Many scientists thus focused on the process of amyloid formation and since the final amyloid formation as observed in vivo could be reproduced in vitro the studies appeared even more relevant (Ahmad et al., 2003). Therefore, the contribution of a host of conditions involving temperature, pressure, nature of environment (oxidative, crowding), metal toxicity in the onset of amyloid formation were hypothized (Bush, 2012; Yamin et al., 2003). These conditions are just a few to mention among the diverse variables that were tired. The sum total of these studies percolated into one theory known as "amyloid cascade hypothesis" (Hardy. and Selkoe., 2002) which proposes following stepwise molecular mechanism

Normal protein → misfolded protein → oligomer → proto-fibril → fibril → plaque.

Out of the intermediate steps shown above, oligomers are considered to be most toxic.

Our lab has been working with many of the proteins involved in above mentioned diseases but we chose to work on standard proteins and especially BSA considering their easy availability and not so well understood amyloid forming pathway.

Table-1			
Property	***Peptide Position***	***Length (AAs)***	***MW Da***
Full length precursor	*1 – 607*	*607*	*69,324*
Signal peptide	*1 – 18*	*18*	*2,107*
Propeptide	*19 – 22*	*4*	*478*
Mature protein	*25 – 607*	*583*	*66,463*

Table-1 and 2: Summarize main properties of BSA

Table-2		
Property	***Values***	***Ref.***
Number of amino acid residues	*583*	
Molecular weight	*66,463 Da (= 66.5 kDa)*	
Isoelectric point in water at 25 °C	*4.7*	(Ge et al., 1998)
Extinction coefficient 279 nm	*43,824 M−1cm−1*	(Peters, 1975)
Dimensions:	*140 × 40 × 40 Å (prolate ellipsoid where a = b < c*	(Wright and Thompson, 1975)
pH of 1% Solution	*5.2-7*	(Putnam, 1975)
Optical Rotation	*$[\alpha]_{259}$-61°; $[\alpha]_{264}$: -63°*	(Putnam, 1975; Sober, 1968)
Stokes Radius (rs)	*3.48 nm*	(Axelsson, 1978)
Sedimentation constant $S_{20,W} \times 10^{13}$	*4.5 (monomer), 6.7 (dimer)*	
Diffusion constant, $D_{20,W} \times 10^{7}$ cm^2/s	*5.9*	(Putnam, 1975)
Partial specific volume, V20	*0.733*	(Putnam, 1975)
Intrinsic viscosity, η	*0.0413*	(Putnam, 1975)
Frictional ratio f/f0	*1.30*	(Putnam, 1975)
Refractive index increment (578 nm) × 10^{-3}	*1.90*	(Putnam, 1975)
Optical absorbance, A279 nm1 g/L	*0.667*	(Putnam, 1975)
Mean residue rotation, $[m']_{233}$	*8443*	(Putnam, 1975)
Mean residue ellipticity: $[\theta]_{209}$ nm;	*21.1*	(Putnam, 1975)
$[\theta]_{222}$ nm	*20.1*	
Estimated α-helix, %	*73*	(Majorek et al., 2012; Putnam, 1975)
Estimated β-form, %	*18*	(Putnam, 1975)

BSA: BSA is bovine form of serum albumin and has been studied in detail for decades. We have summarized many of its characters in the tables below:

BSA is synthesized as a single polypeptide chain of 607 residues out of which the first 18 residues form the signal peptide and residues 19-24 act as pro-peptide that are subsequently cleaved during post-translation modifications leading to formation of a mature bovine serum albumin protein of 582 residues (residues 25-607). Except for Methionine (4 residues) and tryptophan (2 residues) BSA has all other amino acids in bulk amounts. BSA possesses 35 cysteine residues forming 17 disulfide bonds. One cysteine (residue 58 (or 34 when calculating from 25^{th} residue)) does not participate in disulfide and is believed to exist with free -SH side chain (Rombouts et al., 2015). In terms of secondary structure the protein is composed of 31 helices and is predominantly α-helical (71% helix) (Majorek et al., 2012). These helices are often connected with the unstructured regions as mentioned below.

The crystal structure of 66.43 kDa BSA has been solved many a times in free and complexed form. We have used the structure associated with PDB ID 3V03 mostly in this thesis whenever we wanted to refer to the three-dimensional structure of BSA (Majorek et al., 2012). The crystal structure of BSA is often compared to the shape of heart and has been divided into three domains as shown in Fig-i (Curry et al., 1998) Domain-1 extending from residue 24-209; domain-II from 210-402; and domain-III from 403-600. Each domain is further divided into two subdomains A and B. The domains as mentioned above are connected with unstructured chains for example (IA–IB by 106–119; IIA–IIB by 292–315; IIIA–IIIB by 492–511) (Curry et al., 1998). The ligand binding sites of BSA have again been studied in detail and commonly drugs or molecules have been found to bind the sites called Sudlow sites I (in subdomain IIA) and II (in subdomain IIIA) (Sudlow et al., 1975) (as shown in red circles in Fig-i)

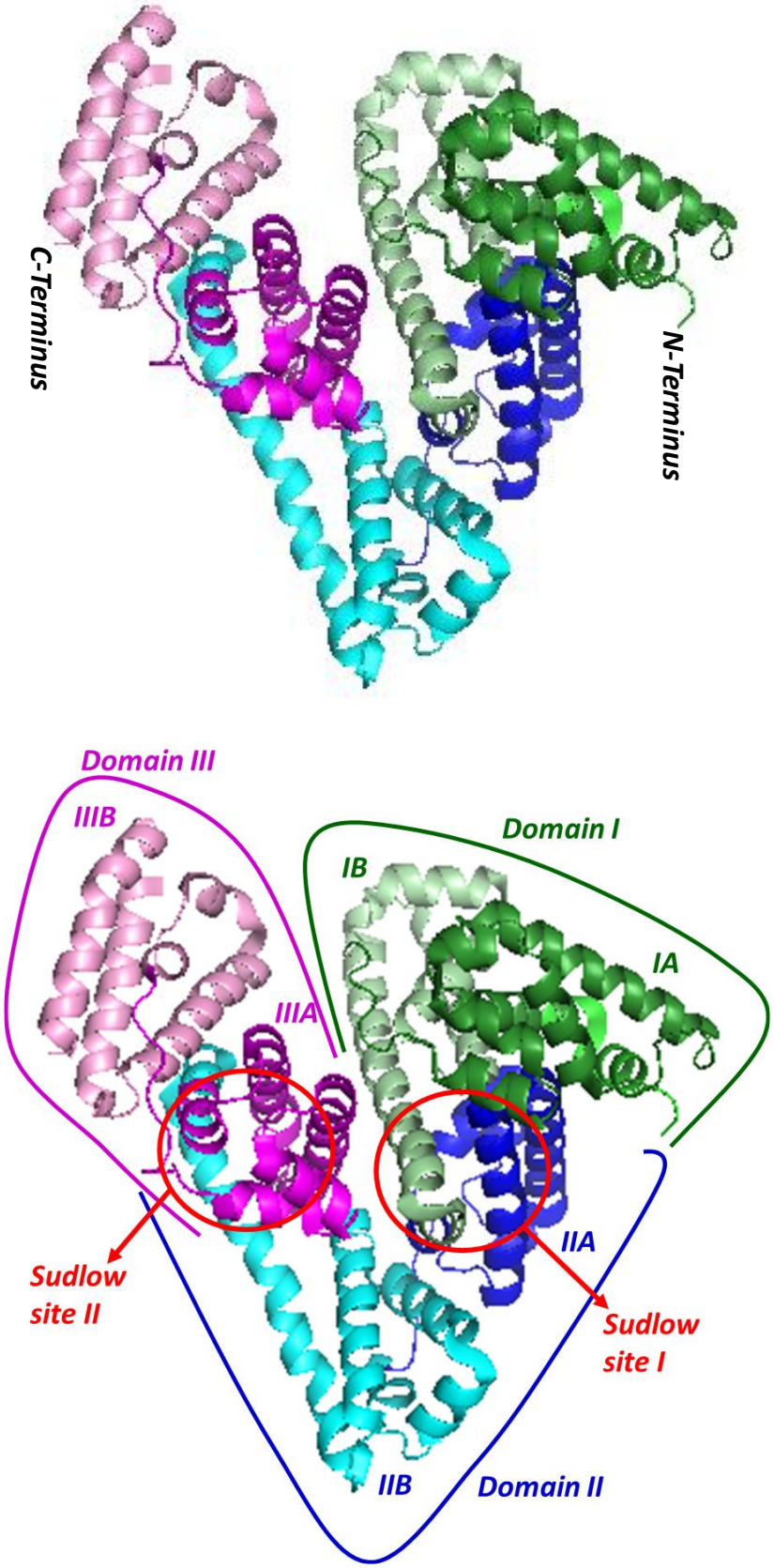

Fig-i Crystal structure of BSA

Location and Synthesis: The major human blood protein, serum albumin (ALB), is encoded on chromosome 4q13.3 by a single-copy autosomal gene (ALB; NCBI Reference Sequence: NG_009291.1). The gene is composed of 15 exons, the last of which is untranslated (Minghetti et al., 1986). In humans, albumin is synthesized (12-25 g/day) in the liver and enters portal circulation immediately (Lundsgaard-Hansen, 1968; Peters, 1975). The protein is secreted into the blood stream, where it accounts for 60%–65% (range 35–45 g/L or ~0.6 mM) of total serum proteins (Peters, 1996a).

The rate of synthesis varies with nutritional and disease states. The liver can increase albumin synthesis to only 2–2.7 times normal because most of the liver's synthetic machinery is already devoted to albumin at rest (Peters, 1996b). The synthetic pathway is common to eukaryotes and is also used for synthesis of other proteins (Moldave, 1985). Albumin synthesis is influenced by many factors, for example, oncotic pressure around hepatocyte, (Oratz et al., 1970; Yamauchi et al., 1992). The decrease in gene transcription or mRNA levels of BSA have been observed to be induced by trauma (Moshage et al., 1987), by inflammation IL-6 and TNF-a (Brenner et al., 1990; Castell et al., 1990), or organic compounds (CCl4) (Peters, 1996b; Peters, 1996c). Diabetics exhibit decreased serum production (Lloyd et al., 1987), which can be cured by insulin treatment (De Feo et al., 1991). Fasting or reducing protein from diet reduces albumin production (De Feo et al., 1992; Sakuma et al., 1987). The levels of albumin can be increased by administration of insulin with steroids (Hutson et al., 1987). The total body albumin pool measures about 3.5–5.0 g kg^{-1} body weight (250–300 g for a healthy 70 kg adult). The plasma compartment holds about 42% of this pool, the rest being in extravascular compartments (Hoye et al., 1972; Mouridsen, 1967).

Functions and interactions of BSA: The main role of albumin in to maintenance of normal colloid oncotic pressure (COP). Critically ill patients exhibited a mean COP of 19.1 mmHg (Weil et al., 1979) while the normal COP is about 25 mmHg through BSA is reported (Gosling, 1995; Traylor and Pearl, 1996; Weil et al., 1979). Albumin is present in the highest concentration among plasma albumins. BSA also helps maintain oncotic pressure maintenance through its negative charge as it helps in retention of positively charged particles. Together these properties help it in having direct effect on fluid distribution in tissues. These facts also indicate importance of albumin administration in critically ill patients (Morisette et al., 1975).

BSA has been found to a variety of molecules and metabolites. Table-3 below shows binding of some molecules to BSA. Sudlow *et al*. have classified drugs into two groups according to two broad binding sites, site I and site II (Sudlow et al., 1975). Site I appears to lie along the long loop of subdomain IIA, extending into the shorter loop (Peters, 1996d). Many different drugs seem to bind here, including salicylates, warfarin, phenylbutazone, indometacin, digitoxin, furosemide, phenytoin, chlorpropamide and some penicillins(Peters, 1996d). Dyes such as sulfobromophthalein, iophenoxate (a radio-opaque dye), methyl red, Evans blue and bromocresol green also bind here, as do endogenous compounds such as bilirubin. Site II is a hydrophobic pocket of residues located in subdomain IIIA (Carter and Ho, 1994). It is responsible for binding compounds such as L-tryptophan, thyroxine (which may also bind at site I), medium-chain fatty acids and chloride. Drugs that bind here include diazepam and other 2,3-benzodiazepines, non-steroidal anti-inflammatory agents that have ionized carboxyl groups (such as ibuprofen and naproxen) and co-fibrillate.

Table-3		
	BSA Interacting partner	***Ref***
1	*1-hexylcarbamoyl-5-fluorouracil (Carmofur) and BSA*	(Hu et al., 2005)
2	*Gemcitabine hydrochloride (GEM) and BSA or HSA*	(Kandagal et al., 2006)
3	*Anticancer drugs (i) 5-fluorouracil (5-FU), (ii) azacitidine (AZ) and (iii) cytarabine (CY) (pyramidine analogues) with BSA*	(Abraham and Mathew, 2014)
4	*Cyanidin-3-glucoside (Cy-3-G) and BSA*	(Shi et al., 2014)
5	*Colchicine and BSA*	(Hua et al., 2005)
6	*Cefixime (CFX) with BSA*	(Zhang et al., 2015)
7	*Diclofenac sodium and BSA*	(Dutta et al., 2006)
8	*Efonidipine with BSA*	(Wang et al., 2008)
9	*Erlotinib hydrochloride and BSA*	(Rasoulzadeh et al., 2010)
10	*Sulfadiazine (SD) binds and unfolds BSA*	(Al-Lohedan and Sajih, 2013)
11	*Nortriptyline hydrochloride (NOT) and promazine hydrochloride (PMZ) with serum albumins*	(Khan et al., 2012)
12	*Mangiferin (MA) and BSA*	(Lin et al., 2009)
13	*Metformin hydrochloride and BSA*	(Tanwir et al., 2012)
14	*Mitoxantrone (MTX) with HSA*	(Khan et al., 2008)
15	*Olmesartan medoxomil and its metabolite olmesartan with BSA*	(Sharma and Pancholi, 2014)

Table-3 Summarizes some BSA or HAS binding molecules.

There are serious ramifications of BSA ligand binding. An allergy to Penicillin has been linked to irreversible coupling of penicilloyl groups to ε lysine groups close to surface of Sudlow site I (Lafaye and Lapresle, 1988). BSA binds NO and interferes with vasodilatory response, acts as anti-coagulant like heparin, maintains microvascular integrity, acts as antioxidant and helps maintain the acid base equilibrium in blood (Carter and Ho, 1994).

BSA is only the second molecule after hemoglobin to exist in more than 100 variants and the sequence of 60% of these mutations is known. Only one of these mutations that binds thyroxine has been found to cause dysalbuminaemic hyperthyroidism (Perlmutter et al., 1986). Analbuminaemia is a condition where no detectable albumin is found in patients and at least 30 such cases have been reported and has been observed to be due to mRNA splicing errors or premature stop codon (Peters, 1996e). The prognostic value of serum albumin concentration is so involved in human health that it has been included in The APACHE III system, and it is more predictive of mortality in critical illness (Knaus et al., 1991).

Data shows patients with a low concentration of albumin after liver transplantation develop toxicity of tacrolimus (FK506) and may benefit from albumin administration. Data from the Netherlands Cancer Institute have shown that patients with peritoneal cancer undergoing prolonged surgery might also benefit from albumin therapy.

BSA Aggregation: Aggregation of BSA and HSA has been reported in variety of conditions. Since BSA and HSA have significant homology, HSA results are often extended to BSA and represented interchangeably. The transformation of HSA from the native form to different conformations has been extensively documented for example;

1. The N (native) to F (fast moving low pH) transition between pH 5.0 and 3.5 involves the unfolding and separation of domain III without significantly affecting the rest of the protein molecule (Dockal et al., 2000). The fibrils formed from this state are characterized by a dramatic increase in viscosity, lower solubility, and a significant loss of helical content.

2. The F-E (equilibrium) transition occurs between pH 3.5 and 1.2, and is accompanied by a further protein expansion with a loss of the intra-domain helices of domain I. In addition, the E form involves an increase in protein intrinsic viscosity and a rise in the hydrodynamic axial ratio from ~4 to 9 (Geisow and Beaven, 1977).

3. The N-B (base, high pH) transition occurs between pH 7.0 and 9.0, with a slight reduction in helical content affecting the two inter-domain helices and a small increase in sheet structure (Khan, 1986).

4. In the presence of denaturant agents, such as urea, HSA shows a two-step, three-state transition with an intermediate (I) characterized by unfolding of the domain III and partial but significant loss of native conformation of domain I (Ahmad et al., 2004a).

The transition to the fibrilar state is not as organized. Different conditions produce fibrils of different size and shape and properties for BSA/HSA. For example, high temperature and time produce different species. As the time of incubation increases at the desired temperature the size of the amyloid aggregate changes from oligomers to mature fibrils. The early fibrilar states are more diffuse but with time these fibrils get more organized and develop sharp contours. Additives affect the aggregation process of BSA as they do for other aggregating proteins. For example, metal ions may induce the amyloid-forming propensity of Aβ, synuclein, insulin and other proteins (Ahmad et al., 2001; Ahmad et al., 2009; Ahmad et al., 2012) which may be of significance in Alzheimer's, Parkinson's and diabetes. Arada et al., observed amyloid fibril

formation from human and bovine serum albumin in the presence of calcium with quasi-simultaneous Fourier-transform infrared (FT-IR) spectroscopy and static light scattering (SLS) (de la Arada et al., 2012). They observed significant Amyloid formation within 1 hr of incubation at 80C in the presence of Ca^{2+}. Bhattacharya et al., transformed the low pH species at higher BSA concentration into amyloid (Bhattacharya et al., 2011). Militello et al., observed that BSA underwent conformational changes during thermally induced aggregation processes loosing most of its tertiary structure and 40% of its helical structure (Militello et al., 2003). The absence of 100% beta sheet in fibril form or intermediate aggregate states was observed to give BSA protection in cytotoxicity experiments (Holm et al., 2007). Juarez et al., observed that diffuse BSA fibrils were formed through intermediate conformational species of BSA/HSA but the fibrils changed morphology with time, pH and buffer conditions (Juárez et al., 2009). The crystal structures of BSA and ESA have been reported (Majorek et al., 2012) and should help to elucidate the mechanistic details of transformation of BSA into its amyloid fibrils.

Challenges in the study of amyloid: A variety of proteins under certain conditions can aggregate and form long, ribbon-like β-sheet rich amyloid fibers, which can be monitored using the amyloid-specific dye ThT (Ahmad et al., 2001; Ahmad et al., 2003; Ahmad et al., 2004b; Ahmad et al., 2005; Ahmad, 2010; Ahmad et al., 2012). The kinetics of this conversion to oligomer, protofibril, and mature fibril can be influenced through an increase in temperature as well as the addition of metal ions and reducing agents. It has been demonstrated with Aβ42 that in physiological ranges, Ca^{2+} greatly reduced the lag time for Aβ42 fibril formation (Acebrón et al., 2008). It appears that this effect is due to the Ca^{2+} ions accelerating the nucleation stage of Aβ42, facilitating the pathway to Alzheimer's fibril formation (Ahmad et al., 2009). Unlike Aβ42,

differential analysis was needed in order to elucidate the exact effect that Ca^{2+} ions on Aβ40 (Muchowski et al., 2000). Through careful and exhaustive analysis, it was possible to deduce strong evidence of 2 mM Ca^{2+} ions affecting Aβ40 through a ~1.4 times increase in rate of fibrillation (Ahmad et al., 2016). Without such treatment of data, such minute differences in Aβ40 kinetics might have been missed due to the drastic difference in kinetic rate between the peptides. This reinforces the inherent value in understanding to the highest possible degree where changes of the protein of interest can be elucidated through the numerous analytical methods. Furthermore, the addition of metal ions to a wide range of protein standards of varying characteristics and the application of the techniques in such studies can be used to obtain a more thorough understanding of possible protein interactions. While it's well documented that ThT serves as a remarkable molecular probe for amyloid (Ahmad et al., 2016), new data treatment and analysis may reveal novel interactions of ThT with native protein as well as oligomer, protofibril and fibril species can further develop the understanding of fibrillation kinetics and protein-ligand interactions. This understanding can then be reapplied to tease out novel approaches in data analysis to further understanding diseases such as AD.

Reducing agents such as dithiothreitol (DTT), tris (2-carboxyethyl) phosphine (TCEP), and β-mercaptoethanol (βME) have also been used in order to alter the native structure of protein, reducing disulfide bonds and exposing nucleation sites within the protein. These disulfide bonds are critical for the correct folding and function of the protein, and are naturally found in more than 50% of amyloidogenic proteins. We demonstrate here the greatly accelerated rate of oligomerization in DTT reduced bovine serum albumin (BSA) which results in mature fibrils through prolonged incubation, as well as try to elucidate the mechanism in which this increased oligomerization and fibrillation occurs as the nucleation sites of BSA become exposed

and accessible for oligomerization. Interactions of DTT with the series of standard proteins is also explored and monitored through ThT fluorescence.

Thioflavin T: Origin and Applications

ThT has been used as tinctorial dye for amyloid detection. ThT is better, simple and efficient technique compared to other technique, namely, Congo-red assay, EM analysis or X-ray diffraction techniques mainly used to detect or characterize amyloid fibrils.

Congo red binding to amyloid appears to have been established by Behold and Divry individually (Bennhold, 1922; Divry and Florkin, 1927) through their observation of yellow-green birefringence produced by amyloid under crossed polarized light in the presence of Congo red. Please refer to Fig-iv for the chemical structure of Congo red. The Congo red technique provided a trove of information about amyloid initially and was considered very useful but later proved to have many draw backs. The assay conditions were detailed soon and it turned out tissue or sample needed to be of certain thickness for birefringence to take place and the need of cross polarizers containing microscope was another limitation that could not be available universally (Elghetany and Saleem, 1988; Westermark et al., 1999). Further, Congo red worked better under conditions with 50–80% ethanol, high salt and alkaline pH conditions to yield binding to amyloid (Puchtler et al., 1962) which did not turn out to be the conditions of choice in many cases.. In addition, Congo red was demonstrated to interact with non-amyloid native proteins (Khurana et al., 2001) besides inhibiting enzymes (Edwards and Woody, 1979) and being influenced by metal ions (Ashburn et al., 1996). Later details also revealed that Congo red can inhibit amyloid formation at high concentration (Feng et al., 2008; Rudyk et al., 2000) but can enhance amyloid formation at low concentrations (Kim et al., 2003). In short concerns about

using Congo red are one too many hence scientist avoid using Congo red when they can. Regardless, the structure of Congo red bound to amyloid has been solved by NMR (Maltsev et al., 2012).

The other technique used for detecting amyloid is X-ray diffraction. Amyloid fibrils produce a characteristic X-ray diffraction pattern with unique arcs in the equatorial and meridional axis (Eanes and Glenner, 1968).

The meridional arc at 4.75Å corresponds to the calculated values of two polypeptide backbones in antiparallel β-sheet lying laterally adjacent to each other (Pauling and Corey, 1953). [Such β-sheets have been referred to as cross beta sheet structures and] for parallel β-sheet this distance is 4.65 Å (Astbury et al., 1935). The 9.8 Å equatorial position corresponds to the spacing of side chain groups in the neighboring polypeptide chains of β-sheets (Kendrew, 1954). However the technique besides requiring the X-ray diffraction set needs the sample preparation and orientation of fibrils in a suitable form. An un-oriented sample will produce a spectra much like shown in the Fig-ii without any useful information.

As reported by Cohen, his group was the first to discover by EM that amyloid from humans had a fibrillar structure (Cohen and Calkins, 1959). Cohen argued that before his discovery the amyloid were thought to be amorphous although cellulose fibrils were identified in 1948 (Shirahama and Cohen, 1967). The diameter of these fibrils was reported to be 100 Å (10 nm).

EM is a comparatively simple technique except the instrumentation may not be available at all facilities. EM has one limitation that is it give snap shots of selective events in the fibrillation process and while it provides the much needed qualitative support it usually is not

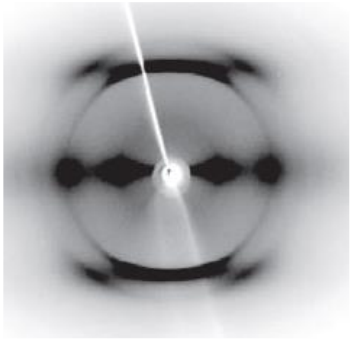

(FEBS J. 2005 Dec;272(23):5950-61. Structures for amyloid fibrils. Makin OS1, Serpell LC.)

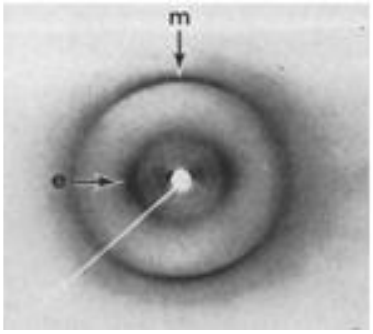

Proc Soc Exp Biol Med. 1969 Sep;131(4):1373-5. Characterization of the amyloid fibril as a cross-beta protein.

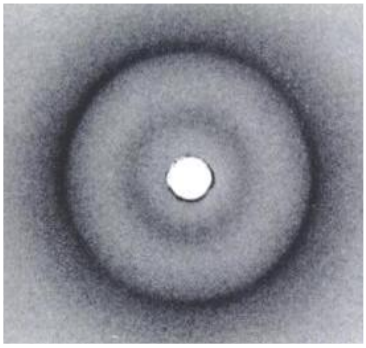

Bonar L, Cohen AS, Skinner MM. J Histochem Cytochem 1968 Nov;16(11):673-7

Fig-ii The reported X-ray studies and diffraction pattern thereof of the amyloid in such studies. The references are provided below each picture

quantitative. EM has been used to provide the mass per unit length of fibrils using the virus controls or modern instrument or computational methods (Chen et al., 2009; Iadanza et al., 2016).

ThT is much user friendly technique than the above mentioned techniques and can provide both qualitative and quantitative data with ease. ThT thus has been widely used in amyloid studies. ThT is a benzathiazole dye used to detect amyloid fibrils. In 1959, Vassar and Culling for the first time demonstrated the use of ThT fluorescent microscopy for amyloid fibril diagnosis in histology (Vassar and Culling, 1959) and the dye has been used extensively in amyloid field since. ThT displays some interesting fluorescent properties. In aqueous solutions ThT displays an excitation and emission maxima of 350 nm and 450 nm respectively. But when bound to the amyloid fibrils both excitation and emission maxima undergo a red shift to 450 nm and 482 nm, respectively. The second interesting thing about ThT fluorescence is its lifetime. There is a single bound connecting the benzothiazole moiety with the benzoamine moiety about which there is an unhinged rotation of the two moieties. This rotation interferes with the dissipation of excitation and emission energies resulting in short fluorescence life time (Sulatskaya et al., 2010). When this rotation is restricted for example during the binding of ThT to amyloid or addition of extra groups to benzothiazole group as in the case of thioflavin S the fluorescence life time improves quantum yield (Sulatskaya et al., 2010).

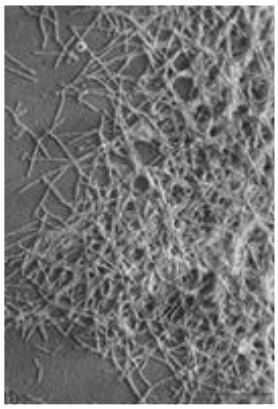

Fig-iii A sucrose-separated preparation of amyloid fibrils shadowed with platinium-palladium (see text). Although a small amount of contamination is found among the packed fibrils, the specimen is quite pure and consists almost solely of amyloid fibrils.)< 70,000 (Shirahama and Cohen, 1967).

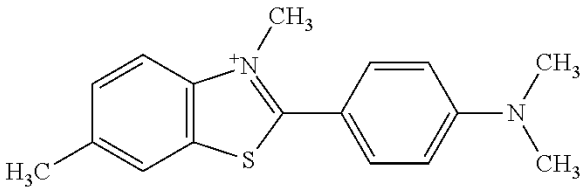

Thioflavin T

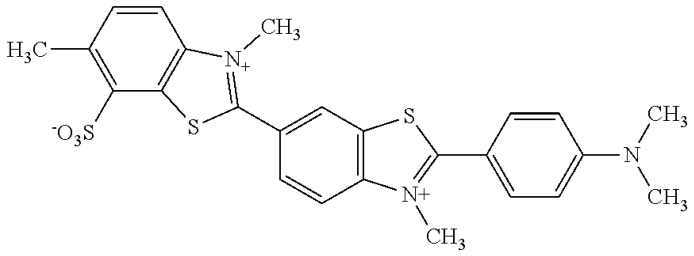

Thioflavin S

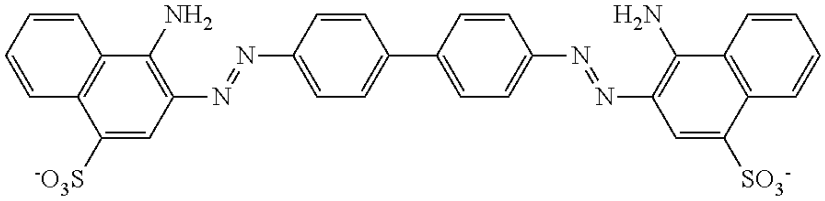

Congo red

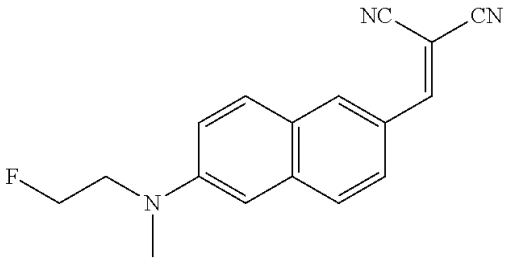

FDDNP

2-(1-{6-[(2-[fluorine-18]fluoroethyl)(methyl)amino]-2-naphthyl}-ethylidene)malononitrile radiotracer used to image neurofibrillary tangles and amyloid aggregates, in living humans through combined use of positron emission tomography (PET)

Fig-iv Various molecules used for amyloid detection

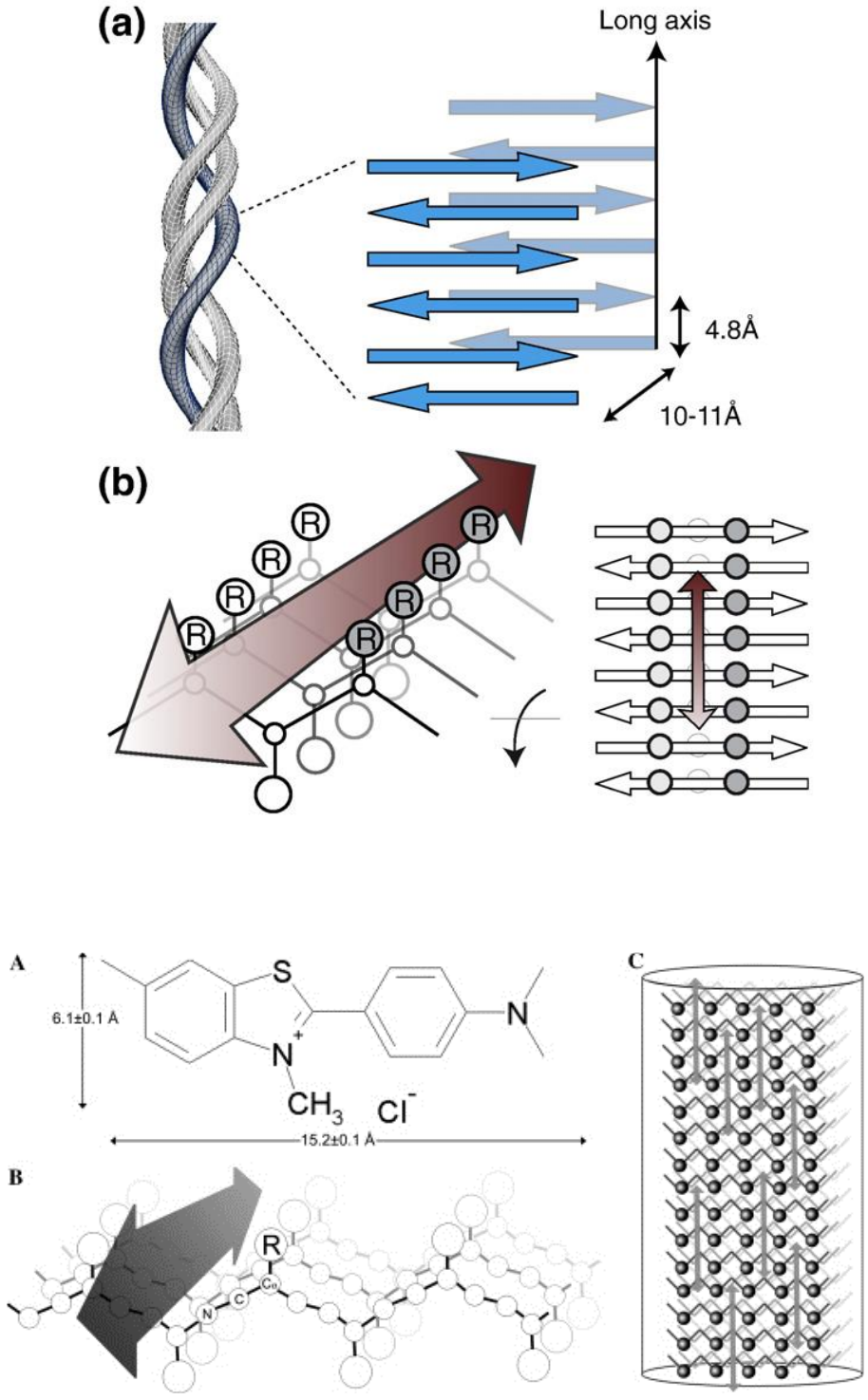

Fig-v The propose mechanism of ThT binding.

The mechanism of ThT binding to the fibrils has been explained as follows. The protein molecules arrange themselves perpendicular to the long axis forming a cross β-sheet structure. This leaves the side chain to extend laterally forming a ladder running parallel to the long axis. Since it lies outside the β-sheet core it is exposed to solvents. It has been proposed using crystallographic and fluorescence polarization data that ThT binds to these solvent exposed side chains and is arranged parallel to the long axis or in other words is held by multiple protein molecules stacked in the amyloid. (Sawaya et al., 2007). This parallel ThT binding model was further shown by the molecular dynamic simulations (Wu et al., 2008).

Peptide self-assembly mimics (PSAMs) were further used to elucidate the mechanism of ThT binding (Biancalana et al., 2008). Based on the results and the molecular dynamic simulations of PSAMs it was established that ThT binds in the lateral pockets caused by the aggregating peptides and lies perpendicular to the long axis of fibrils (Wu et al., 2009). ThT molecules were found stretched in a longitudinal translation across the five Leu and Tyr residues and lacked any preferred orientation. This space (Cα–Cα distance of a four residue ladder ∼14 Å) appears to be longer than the longitudinal length of ThT (∼15 Å) (Biancalana et al., 2008; Wu et al., 2009). These data explain the affinity of ThT towards the amyloid fibrils and why this dye has been so successful in its use as tinctorial dye for amyloid detection.

Proteins may bind to ThT in a variety of ways. ThT has been observed to bind non fibrilar proteins, such as acetylcholinesterase, a largely helical protein (Harel et al., 2008). The binding has again been possible due to interactions with aromatic residues like Tyr and Trp resulting in the formation of a hydrophobic pocket. In addition ThT binding to the amyloid fibrils can be interfered by rifampicin, glycerol, PEG and bis-ANS, resveratrol and curcumin reviewed in (Biancalana and Koide, 2010).

With this information we set to study the interaction of ThT with different proteins.

Main aims of the thesis project:

Aim-1: First and foremost to reproduce the amyloid behavior of BSA and other similar proteins in our experimental conditions so that we can study ThT effects.

Aim -2: To explore and characterize the binding aspects of ThT with different proteins especially BSA.

Aim-3: To explore the effect of ThT binding on the protein secondary structure and stability.

Aim-3: To locate the ThT binding site by X-ray crystallography or computer simulations.

Aim-4: To explore the extent of generalization of ThT binding among the ThT-binding proteins.

Material and Methods:

Preparation of Protein Stock

Lyophilized proteins were purchased from Sigma Aldrich. Solutions were prepared by weighing protein powder on the scale and dissolving in double distilled water. Concentration of protein solution was determined using nanodrop or spectrometer using extinction coefficients reported in the literature. The extinction coefficients and have been mentioned here for reference [Ovalbumin 30590 $M^{-1}cm^{-1}$, Alcohol Dehydrogenase 47530 $M^{-1}cm^{-1}$, Lysozyme 38940 $M^{-1}cm^{-1}$, Myoglobin 13,940 $M^{-1}cm^{-1}$, Insulin 16960 $M^{-1}cm^{-1}$, Proteinase-K 36580 $M^{-1}cm^{-1}$, Trypsin 37000 $M^{-1}cm^{-1}$, RNase A 9416 $M^{-1}cm^{-1}$, BSA 43,824 $M^{-1}cm^{-1}$]. In each case an average value from triplicate readings was taken to ensure protein concentration was measured accurately. This method was uniformly applied to all proteins used in this study with their respective extinction coefficients to guarantee consistency.

Protein concentrations were also measured using Pierce protein assay and Bradford assay. BSA was used as standard protein in these assays and its concentration was measured on the spectrophotometer [using extinction coefficient 43,824 $M^{-1}cm^{-1}$]. The data in the linear range, was used to calculate the concentrations of the other proteins samples. It was determined that nanodrop and spectrometer methods were as accurate in determining protein concentration and as reliable.

Stock protein solutions were aliquoted out and stored at -20 °C, and used within one week to ensure maximum sample quality. These stored aliquoted protein samples were thawed for the intended experiment just once and leftover protein solution was discarded to prevent

repeating freeze/thaw cycles. In general, experiments were carried out in 20 mM pH 7.4 phosphate buffer unless stated otherwise.

Size Exclusion Chromatography (SEC)

BSA at 2 mg/mL (30 µM) was incubated at 60 or 80℃ for varying times in an Eppendorf tube. After incubation the protein samples were centrifuged at 20,000 rpm for 10 minutes on a table top Eppendorf microfuge before loading 100 µL supernatant on a LKB TSK G3000 SW 8x300mm size exclusion column using a Pharmacia P-500 FPLC pump at a flow rate of 1 mL/min. The column was pre-equilibrated with buffer [20 mM pH 6.8 phosphate with 0.05% sodium azide] by at least three column volumes. Results were recorded at 280 nm by LDC Analytical Spectromonitor 3200 and charted at a speed of 1 cm/min. Data traces thus obtained were digitized using WebPlotDigitizer v3.1 (http://arohatgi.info/WebPlotDigitizer/) and replotted in sigma plot or MS excel.

SDS-PAGE

Protein samples were added to laemmli sample buffer (1:1) and separated mostly on a 9% acrylamide gel at room temperature for one hour at 150 mV with a 4% stacking gel unless stated otherwise. Gels were stained with Coomassie brilliant blue dye R-250 0.1% prepared in 40% MeOH and 60% double distilled water. Gels were destained with a solution of 10% acetic acid, 40% MeOH and 50% double distilled water. The buffer used was standard pH 8.3 Tris-Glycine-SDS electrophoresis buffer.

Thioflavin T (ThT) Fluorescence Changes

Protein solutions were made with a concentrations between 10 and 50 µM using above described method and then incubated at 80 °C. Aliquots were taken out at desired time intervals and added to 200 µL of 20 µM ThT unless stated otherwise. Fluorescence was measured on a TECAN infiniteM200 Pro plate reader with the following parameters; Ex=444 nm, Em=495 nm. Scan of emission range was taken from 480 to 530 nm. ThT stock solution was prepared in double distilled water and concentration was determined using an extinction coefficient of 36,600 $M^{-1}cm^{-1}$ at 412 nm ((Groenning, 2010)).

Transmission Electron Microscopy (TEM)

Negative staining EM studies were carried out on Philips (FEI) CM12 Transmission Electron Microscope. BSA 2 mg/mL (30 µM) in the presence or absence of 15.5 mM DTT was incubated at 80 °C for 30 days and 5 µL samples of selected time points were applied to Formvar-filmed 400 mesh copper grids (Ted Pella Inc., CA) for two minutes. Sample was wicked off with Kimwipes and the grids were washed 5 times with double distilled water. Each time 5 µL double distilled water was applied to the grid and wicked off gently but immediately with kimwipes. The grids were finally washed 2 times with 2% uranyl acetate solution (solutions wicked off following each wash). The residual uranyl acetate on the grids following last wash was left to dry. TEM images were taken using software provided with the machine and reprocessed in Adobe Photoshop Version: 13.0.1 whenever needed.

Intrinsic Fluorescence Measurements

Fluorescent amino acids (tryptophan and tyrosine) were used as intrinsic markers wherever possible. Protein samples were selectively measured for intrinsic tyrosine fluorescence on TECAN infiniteM200 Pro plate reader by using exciting wavelength at 280 nm, and recording emission between 280 to 340 nm.

Far and Near Ultraviolet (UV) circular dichroism (CD) Measurements

CD spectra were recorded on an Aviv 202 circular dichroism spectrometer at Department of Biochemistry, Duke University. The spectra were recorded in a 1 mm path length cell at 25 °C. Far UV spectra were recorded between 200 nm to 275 nm with 0.5 sec wait time, 0.2 sec averaging time, 1.0 nm bandwidth and with 0.50 nm step size. Blank for CD measurements was 20 mM phosphate buffer pH 7.4 in double distilled DI water. For far-UV CD samples were made by taking each protein at 0.5 µM final protein concentration in 20 mM phosphate buffer, pH 7.4 and varying concentrations ThT ranging from 0 to 50 µM unless stated otherwise. To account for the buffer and ThT contribution in this region, the far UV-CD spectra of ThT only in the buffer was also recorded at each ThT concertation. The spectra thus obtained were subtracted from the far UV-CD spectra of protein + ThT samples

Near UV-CD measurements were carried out in similar manner with varying ThT in phosphate buffer but with following differences. The protein concentration used in near UV-CD was 50 µM and the data was recorded over the wavelength range of 250 nm to 475 nm.

Far UV-CD Protein thermal melts

For getting information about melting points (Tm) change in CD was recorded at a single wavelength in the temperature range of 25 to 90 °C on an Aviv 202 circular dichroism spectrometer. The spectra were recorded in a 1 mm path length cell with a starting temperature of 25 °C and the temperature was varied with increments of 1 °C/min until the final temperature of 90 °C was reached. The data was recorded using a bandwidth of 1 nm, equilibration time of 0.80 minutes and an averaging time of 0.50 seconds unless stated otherwise. Wavelength used to monitor change in ellipticity was 222 nm. Temperature was cooled down to 25 °C manually in stepwise manner by altering cell temperature 5 °C at a time per ten minutes to minimize cuvette changes to birefringence that could upset reproducibility in samples. Protein concentrations used in these thermal melts was 0.5 µM and three melting curves were recorded for protein only; protein + 10 µM ThT and protein + 30 µM ThT.

Molecular Docking by Auto-Dock

BSA crystal structure parameters were downloaded from Protein Data Bank (PDB) (ID: 3v03) (www.rcsb.org). Monomer BSA was extracted from PDB file via Vi text editing software (Schröder et al., 1993). Similarly, ThT structure was generated through the isolation of the ligand structure from another PDB structure (PDB ID: 3EC5) using Vi text editing (Singleton et al., 2003). Autodock 4.2 was used to set up BSA and ligand ThT with all hydrogens being added simultaneously (Polymeropoulos et al., 1997). Gasteiger charges were assigned to the protein and flexible ligand to evaluate ligand binding energies over conformational search spaces using the Larmarkian genetic algorithm (Spillantini et al., 1997). Binding sites for ThT were obtained

through a series of steps involving isolating specific fragments of BSA to serve as search area (through use of Vi text software and PDB file) as well as searching the complete monomer and dimer crystal structure. Out of the generated binding modes, minimum energy conformation states of the ligand bound protein were used to predict potential binding sites. The identification of these binding sites relied on conformational overlap of ThT through repeated trials with BSA fragments, monomer and dimer so that confidence in suggested binding sites could be obtained. Confidence in method was reached through reproduction of previously studied ligand binding conformations by other groups in our lab and within the computational parameters described above.

Protein Crystallography

BSA was crystallized using hanging drop method. Protocol for producing crystals was followed as has been reported in the case of PDB ID 3v03 (Schröder et al., 1993). 500 µL of reservoir buffer with 20% PEG 3350 w/v and 0.2 M calcium acetate in 0.1 M Tris HCl buffer, pH 6.5 was placed in the reservoir wells. The buffer was sterilized by passed through 0.2 µM filter. Three BSA samples were made and each mixed 1:1 with the reservoir buffer in a final volume of 10 µL. The stock BSA solution was prepared such that they final concentrations in the drop reflect 20 mg/mL (300 µM) BSA + 0 µM ThT; 20 mg/mL (300 µM) BSA + 10 µM ThT; or 20 mg/mL (300 µM) BSA + 30 µM ThT. Three drops of each sample mixed with reservoir buffer were placed on a R3-231 22 mm x 0.22 mm siliconized cover slip (Hampton Research, USA) and placed on the wells of VDX 24 well plate (Hampton Research, USA) the rims of which were coated with Dow Corning vacuum grease (Hampton Research, USA) for efficient sealing. The plate was incubated in a constant 16°C incubator and crystal growth monitored by Olympus SZX7 Stereo Light Microscope with X-Cite Series 120 Q twice a week for three weeks.

Results:

1. Initial protein analysis and Reproducing BSA aggregation behavior

As mentioned in preceding sections we first checked the purity of the protein we were going to work with. We loaded 20 uL of 30 μM BSA in 20 mM phosphate buffer pH 7.4 on 9% SDS PAGE and ran it under denaturing conditions. As shown in Fig-1, the native protein band was observed around 66 kDa with respect to standard markers. The protein appeared to move as a single band and without any aggregates. But under similar conditions, BSA with 15.5 mM DTT moved slower than its native form but again as a single population and without any significant amount of aggregates. The molecular weight of this band corresponded to ~80kDa. The important thing to note here was that in the presence of DTT the protein did not dimerize or multimerize but instead appeared to have lost its compactness and structure which is not a surprise given the abundance of disulfide bonds in this protein. We have described more of it in Fig-3 below. We want to mention here one deviation we opted from standard SDS protocol. We did not heat the samples to 100 °C before loading on the gel. This was mainly done to be able to ascertain the effect of temperature on BSA in subsequent experiments.

Next we monitored effect of temperature on BSA. BSA was incubated for 2 hours at room temperature (RT) or at 80 °C and in the presence and absence of 15.5 mM DTT in 20 mM phosphate buffer pH 7.4 as shown in Fig-2. The results of BSA in the presence or absence of DTT described above were reproduced in lane 3 and 4 (Fig-2). After 2 hours of incubations at 80 °C BSA in the presence of DTT (lane 1) exhibited a decrease in the band intensity. Under equal and similar experimental conditions this could be because of less protein entering the gel as a consequence of higher order aggregate formed during the incubation time at 80 °C. Supporting of this conclusion, we observed BSA incubated without DTT also exhibited decreased intensity

of its main band at 66 kDa but in addition and unlike DTT included sample a number of higher order aggregates were observed. It is noteworthy that in the absence of DTT there is coexistence of different but gel penetrable aggregates perhaps in equilibrium but in the presence of DTT the equilibrium if shifted mostly to larger gel impenetrable aggregates.

In the case of aggregation and amyloid type in particular, the oligomerization has been observed to be preceded by the at least partial unfolding of the protein. We wanted to confirm the higher order oligomers observed in the absence of DTT (Fig-2) were formed through this process and that DTT treated samples were infact partially unfolded to start with. We used limited proteolysis to access the conformational changes if any that occurs in molecule with DTT or high temperature treatment and with the treatment involving both temperature and DTT. The results have been summarized in Fig-3. BSA was first incubated for 2 hours at either 80 °C or RT in the presence or absence of 15.5 mM DTT. The samples were taken out and incubated further at RT for additional 30 minutes in the presence or absence of proteinase K. Proteinase K was added in 1:100 w/w proteinase:protein ratio. Samples were loaded on 11% SDS PAGE to identify any smaller fragments produced by proteolysis. At RT, addition of proteinase K did not appear to cause proteolysis of BSA either in the presence (lane 3) or absence (lane 4) of DTT. At 80 °C, complete proteolysis of the BSA incubated for 2 hours was observed (lane 5). A smear corresponding to low molecular weight was observed in this case which indicates that BSA molecules under these conditions are unfolded and the proteolytic sites become exposed and easily cleavable. However, in the absence of DTT at 80 °C, a smear corresponding to high molecular weight and low molecular weight species was observed. Production of low molecular weight fragments could be explained as above but higher order fragments and species could be explained in two ways. In one scenario some of the BSA species may assemble in a manner that

makes some proteolytic sites inaccessible resulting in limited proteolysis and larger fragments. In the second scenario the fragments produced in absence of DTT after incubation at 80 °C might be in conformationally distinct structures due to intact disulfides which might favor aggregation and result in the formation of higher order species.

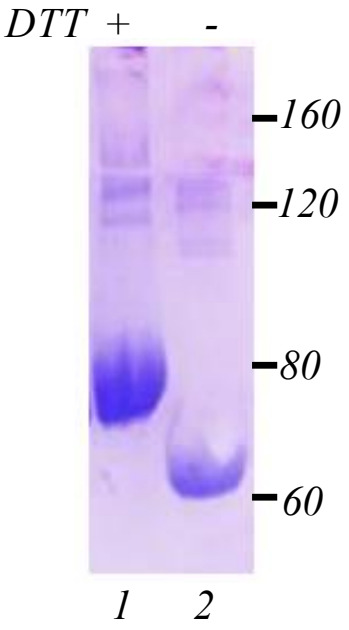

Fig 1. BSA run on 9% SDS PAGE in the presence (lane 1) and absence (lane 2) of 15.5 mM DTT. Figure shows the purity of BSA protein preparations, BSA moves as single band and addition of DTT does not lead to dimerization of BSA. Samples were made in 20mM phosphate buffer pH 7.4 and incubated for 2 hours at mentioned temperatures. BSA concentration was 30 μM.

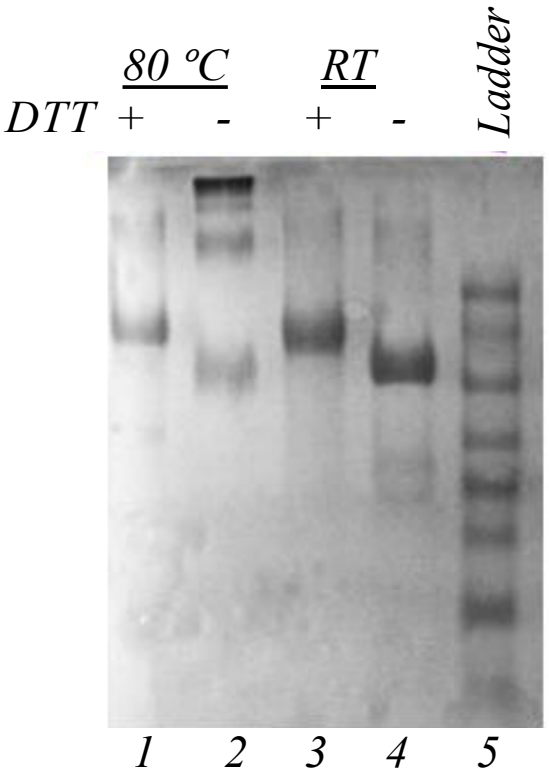

Fig 2. BSA run on 9% SDS PAGE under different conditions - Lane 1, in the presence of DTT at 80 °C; lane 2, in the absence of DTT at 80 °C; lane 3, in the presence of DTT at room temperature (RT); lane 4, in the absence of DTT at RT; and in lane 5, molecular weight markers were run. Each sample was incubated for 2 hours under its particular condition before loading on the gel. Figure shows at 80 °C (lane 1 and 2) most of the protein does not enter the gel leading to faded bands. Samples were made in 20mM phosphate buffer pH 7.4 and incubated for 2 hours at mentioned temperatures. BSA concentration was 30 μM.

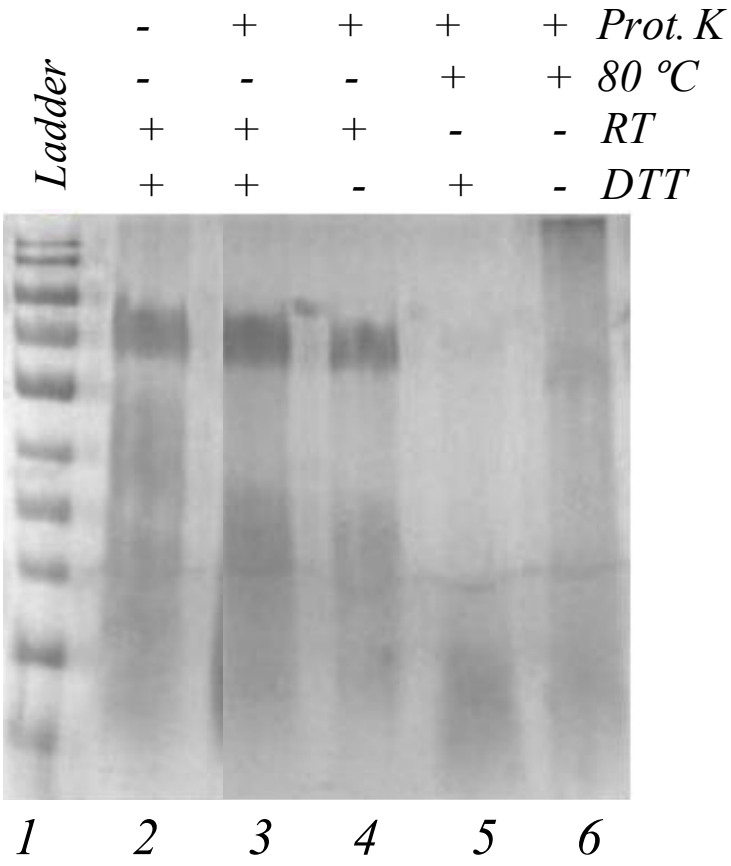

Fig 3. BSA run on 11% SDS PAGE under different conditions - Lane 1, standard markers; in the presence of DTT at 80 °C; lane 2, BSA incubated the presence of in the absence of 15.5 mM DTT at room temperature (RT); lane 3, BSA incubated at 80 °C in the presence of DTT, and then treated with proteinase K for 30 min; lane 4, BSA incubated at RT and then treated with proteinase K; lane 5, BSA incubated at 80 °C with 15.5 mM DTT and then treated with proteinase K; lane 6, BSA (30 μM) incubated at 80 C and then treated with proteinase K. Each sample was incubated for 2 hours under its particular condition before loading on the gel. BSA concentration was 30 μM, buffer used was 20mM phosphate buffer pH 7.4; DTT was 15.5 mM; proteinase K final amount was 1:100 w/w with respect to protein concentration.

Size exclusion chromatography (SEC): *reproducing the aggregation pathway of BSA.*

As mentioned in the introduction the amyloid cascade hypothesis (Hardy. and Selkoe., 2002) suggests that proteins transform into amyloid in steps trigged by protein conformational changes that follows association of molecules into oligomers that combine together to form protofibrils. More than one protofibril combines to form a mature fibril. This process has not been detailed for BSA but because of BSA-amyloid being produced under the lab conditions (Bhattacharya et al., 2011) initial oligomerization is highly predicted.

To investigate this process we incubated 30 □M BSA for varying time periods at 80 °C and analyzed the products on SEC G2000 column. The void volume of column was found to be ~4 mL based on the elution of blue dextran and the inclusive volume was found to be 20 mL based on elution of tryptophan-amide. Next a series of samples of BSA incubated for various time intervals was loaded on the column. All the samples were centrifuged at 13000 rpm before loading on the column to prevent clogging.

Control BSA (0 hours) showed a profile with a large peak eluting at about 8.7 mL (Fig-4). This profile also exhibited a small amount of BSA dimer eluting at about 7.4 mL. Sample incubated for 0.16 hours (10 min) indicated that most of the BSA was converting into various oligomeric species with dimer as the major species. The profile also exhibited a larger (protofibril) peak eluting at 4.8 mL. A 20 minute incubation (0.33 hours) at 80 °C resulted in shift of equilibrium towards higher oligomers. The protofibril peak appeared still distinct at this point and its concentration appeared to have increased. Further increase in incubation time resulted in gradual conversion of oligomers to higher molecular weight forms. The protofibril peak at 1 hour of incubation appeared as a shoulder indicating the molecules were organizing into more uniform species, which could be expected to be kinetically and thermodynamically

stable. BSA finally seemed to exclusively exist in protofibril form after 7 hours of incubation at 80 °C. The protofibril specie was observed to be very stable as it sustained even after 96 hours of incubation at 80 °C without any significant loss in amount.

The SEC series of experiments on BSA was repeated in the presence of 15.5 mM DTT as shown in Fig-5. We have re-plotted the profiles of 0 hr and 96 hr obtained in the absence of DTT from Fig-1 for easy comparison of the results. In the presence of DTT and within 10 minutes of incubation at 80 °C BSA was predominantly and uniformly converted into the proto fibrilar species. A single peak eluting just above void volume within 10 minutes of incubation at 80 °C was observed in this case that matched with the peak obtained after 7-96 hours of incubation in the absence od DTT. This indicated that the aggregation process is facilitated by the reduction of disulfide bonds in such a way that the formation of intermediate oligomers was kinetically very fast or completely skipped under these conditions. This could be explained on the lines that addition of DTT and reduction of disulfides alters the conformation of BSA leading to the exposure of amyloid nucleating sequences. Once exposed their interaction could be facilitated and thus be kinetically more labile and undetectable within the transition time of SEC partition coefficient. The experiment was repeated with different reducing agents like BME and TCEP with similar results (data not shown) and thus favoring the reason derived above. Fig-5 also exhibits the SEC profiles obtained at 36 hours and 48 hours superimposed on each other indicating the reproducibility of the results. As observed in the case of BSA incubated in the absence of DTT, BSA incubated in the presence of DTT showed constant existence of the protofibrilar species even after 96 hours of incubation at 80 °C.

Fig 4. Size exclusion chromatography (SEC) of BSA under different conditions – Figure summarizes SEC profiles obtained by loading BSA incubated for various times at 80 °C on G2000 column incubated for desired times. The time of incubation for each profile is shown against each profile. The data indicates stepwise oligomerization of BSA under these conditions. Each sample of 30 μM BSA was prepared in 20mM phosphate buffer pH 7.4 for different times and loaded on column after centrifugation.

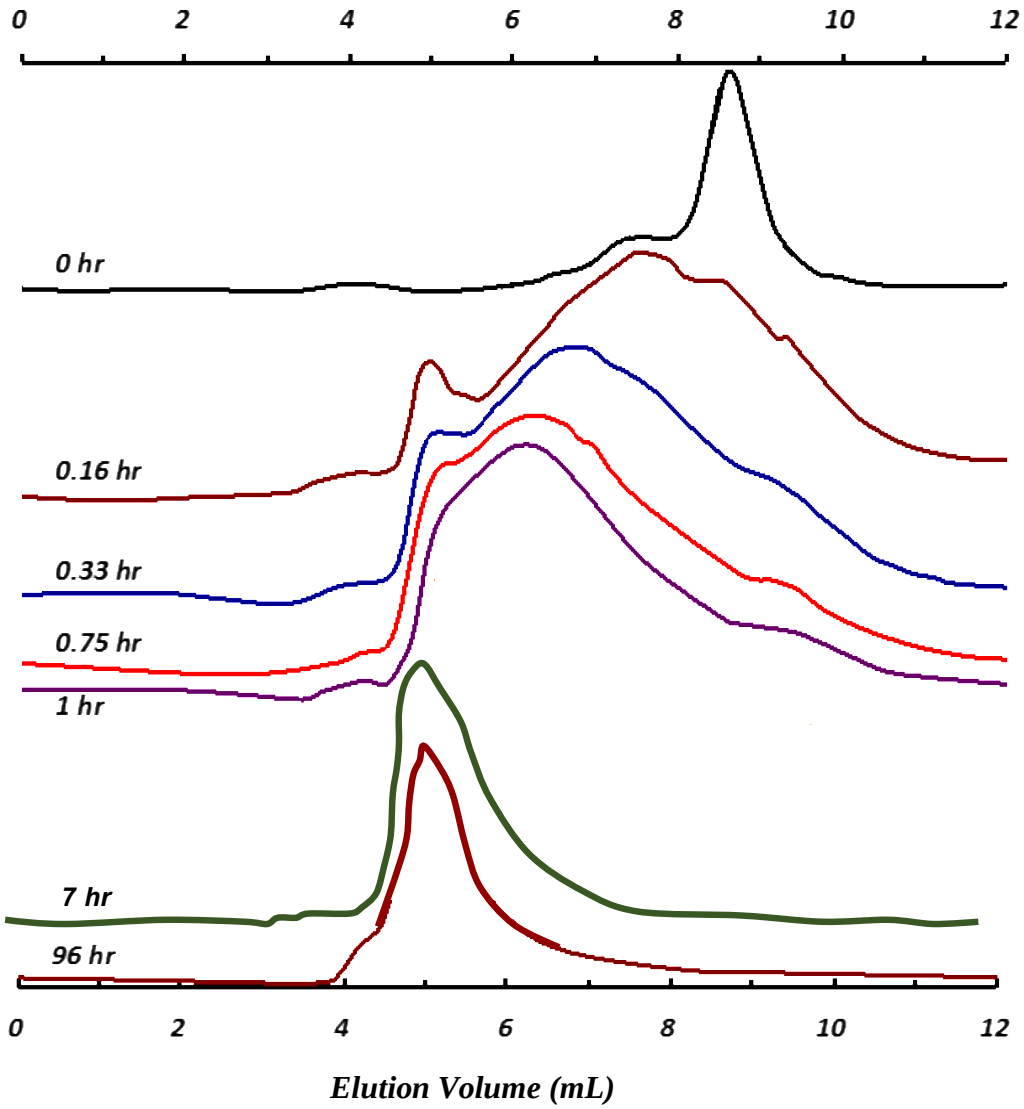
0
2
4
6
8
10
12
0 hr
0.16 hr
0.33 hr
0.75 hr
1 hr
7 hr
96 hr
Elution Volume (mL)

Fig 4.

Fig 5. Size exclusion chromatography (SEC) of BSA with DTT and under different conditions – Figure summarizes SEC profiles obtained after loading BSA incubated with 15.5 mM DTT for various times at 80 °C on G2000 column. The time of incubation for each profile is shown against each profile. Top two profiles with labels 0 hr and 96 hr are from Fig 4 replotted here for comparison. Two more profiles obtained at 36 hr and 48 hr in the presence of DTT have been superimposed to emphasize the reproducibility of data. The data indicates loss of intermediate steps in oligomerization of BSA in the presence of DTT during this monitoring under these conditions. Each sample of 30 μM BSA was prepared in 20mM phosphate buffer pH 7.4, incubated for different times at 80 °C and loaded on column after centrifugation.

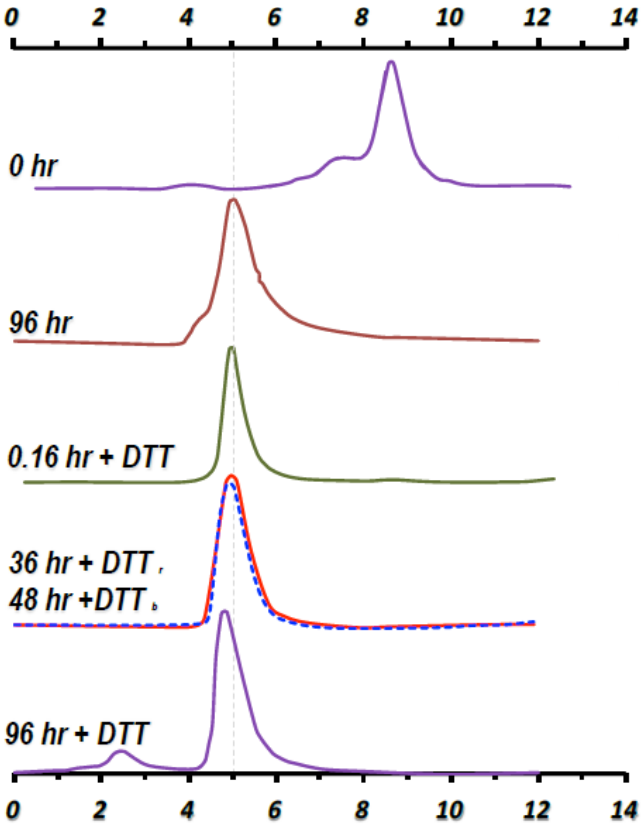
0
2
4
6
8
10
12
14
0 hr
96 hr
0.16 hr + DTT
36 hr + DTT ,
48 hr +DTT ,
96 hr + DTT
0
2
4
6
8
10
12
14
Elution volume (mL)

Fig 5.

Electron Micrography (EM) studies of BSA:

As mentioned in the introduction EM is one of the primary techniques along with Congo-red and X-ray diffraction used to confirm the presence of amyloid (Ahmad et al., 2003; Ahmad et al., 2004b). This has been applied to BSA and again to confirm we were studying the same amyloid process we carried out EM analysis of BSA under the condition we were using. These EM results have been summarized Fig-6.

BSA (30 μM) was incubated in the presence and absence of 15.5 mM DTT at 80 °C and aliquots were drawn at different time intervals. Five uL of the aliquot was loaded on coated copper grids and negatively stained as mentioned in material and methods. The EM picture of BSA incubated for 2 hours in the absence of DTT (Fig-5 Panel A) exhibited rounded structures 5-15 nm in diameter. These structures have been previously compared to oligomeric species for other amyloid forming proteins (Ahmad et al., 2009; Kayed et al., 2003). Unlike this, BSA incubated in the presence of DTT did not exhibit any oligomers but instead the long and mature fibrils (with ~ 20 nm width) were predominant in the EM pictures (Fig-5 Panel B). These data align with the results of our SEC studies. The samples here were not centrifuged as in the case of SEC and that is not interfering with the mechanism is evident from these results. Furthermore, we carried out EM studies on extensively incubated BSA (22 days) in both the conditions. The EM of BSA in absence of DTT exhibited what is termed as “spaghetti type” amyloid fibrils in that they are abundant, loose, puffed and do not possess stretched segments or sharp edges (Fig-5 Panel C). In comparison, BSA incubated with DTT exhibited sharp and stretched fibrils after 22 days of incubation at 80 °C.

These data therefore served as a proof for us that BSA under our condition was aggregating to form amyloid following the mechanism widely accepted by the scientific

Fig-6 Electron Micrography (EM) analysis of BSA: Figure shows EM pictures of BSA incubated at different time intervals at 80 °C. Panel A, EM picture of BSA incubated at 80 °C for 2 hours; Panel B, BSA incubated for 2 hours at 80 °C in the presence of 15.5 mM DTT; Panel C, BSA incubated at 80 °C for 22 days; and Panel D, BSA incubated for 22 days at 80 °C in the presence of DTT. The protein concentration was 30 μM in each in 20 mM phosphate buffer pH 7.4

A

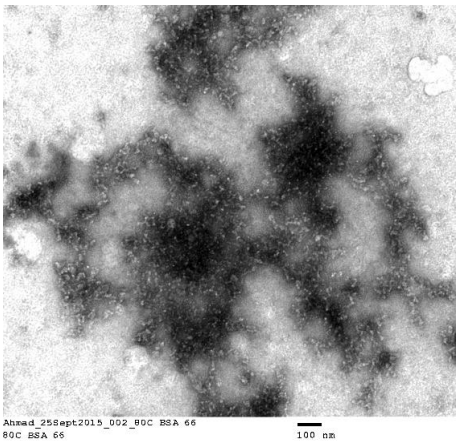
Ahmad_25Sept2015_002_80C BSA 66
80C BSA 66
100 nm

B

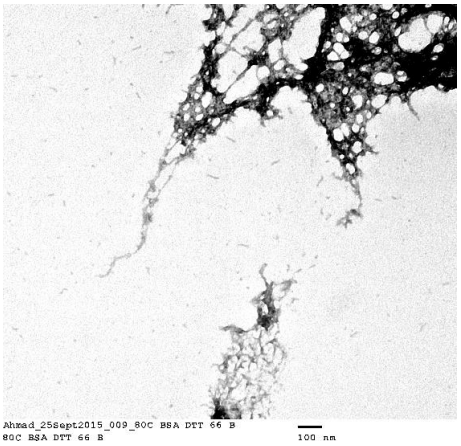
Ahmad_25Sept2015_009_80C BSA DTT 66 B
80C BSA DTT 66 B
100 nm

C

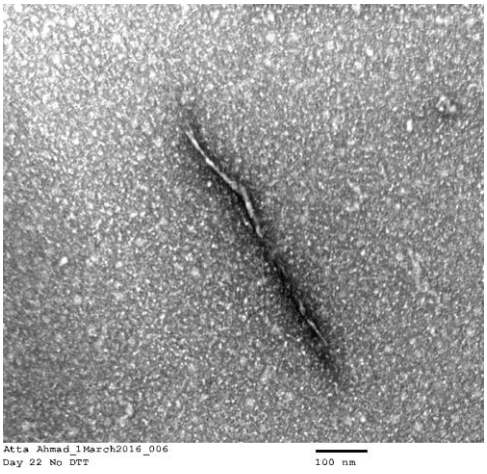
Atta Ahmad_1March2016_006
Day 22 No DTT
100 nm

D

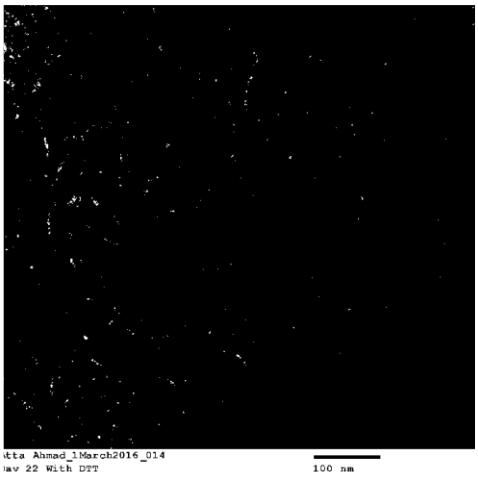
tta Ahmad_1March2016_014
ay 22 With DTT
100 nm

Fig-6

community (Ahmad et al., 2005; Hardy. and Selkoe., 2002; Kayed et al., 2009). The differences observed with DTT treatment were interesting we followed them further but are not relevant to the topic we are describing in this thesis. Again, as mentioned in the introduction/section amyloid detection is easier to follow by ThT fluorescence based on its sensitivity and efficiency. It is during this process that we observed ThT binding of BSA and extended it to the studies of other proteins.

ThT fluorescence changes with different proteins:

ThT fluorescence changes on binding in that it is excited at 444 nm and it emits around 490 nm. Fibril obtained from BSA at 30 μM incubated at 80 °C was treated with different concentrations of ThT to get a better insight of signal to noise ratio in the case of ThT fluorescence with respect to fibril. But the control native run along side gave interesting results complied in Fig-7A. The fluorophore was excited at 444 nm and at low concentrations no ThT binding was observed but instead a background signal emitting weakly around 524 nm was observed. As the concentration increased ThT exhibited binding to the native BSA, which was not expected. As shown in Fig-7A native BSA produced an excellent binding curve with emission maxima at 495 nm. We decided to study the behavior of increasing concentration of ThT with BSA or different proteins. The experiment was carried out with BSA and Ovalbumin first (Fig-7B) each at 15 μM concentration. For Ovalbumin a sharp increase in ThT fluorescence at 492 nm until about 15 μM ThT was observed. From 15 to 50 μM the ThT fluorescence plateaued. For BSA a gradual increase in ThT was observed up to 30 μM ThT after which it leveled. An experiment with protein concentration at 30 μM showed similar results only saturating at twice the TnT concentrations (data not shown). From these data it appears that ovalbumin binds to ThT in a 1:1 ration and with

Fig-7 ThT fluorescence changes with native proteins: Panel A; BSA at 15 uM was treated with either 2 uM ThT or 50 uM ThT and fluorescence was measured after exciting at 444 nm. 2 uM ThT containing sample exhibits fluorescence characteristic of unbound ThT with emission maximum around 515 nm. 50 uM ThT containing sample exhibits fluorescence characteristic of bound ThT with emission maximum around 490 nm. Panel B, shows changes in ThT fluorescence at constant BSA or ovalbumin concentration (15 uM) and increasing ThT concentration. Both studies were carried out in phosphate buffer pH 7.4 at room temperature.

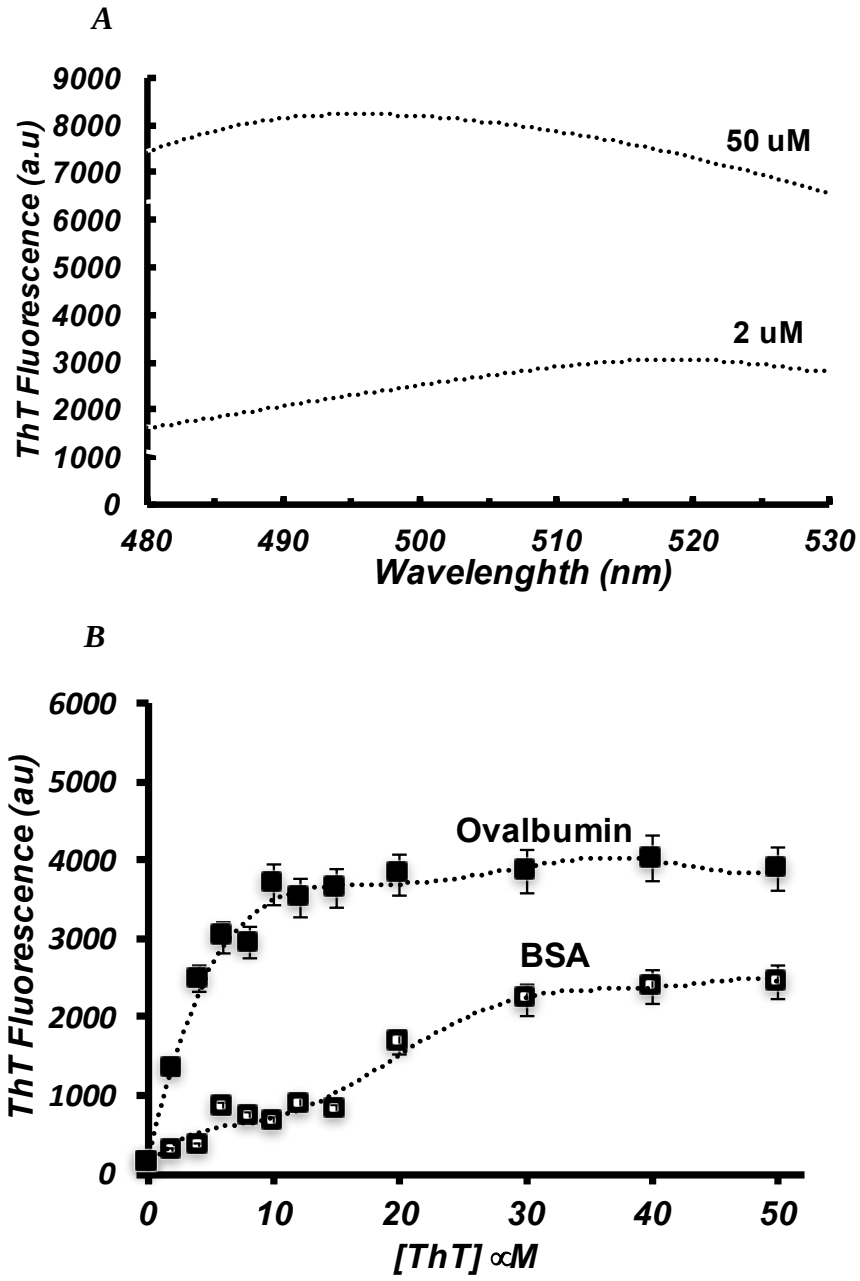
A
9000
8000
7000
6000
5000
4000
3000
2000
1000
0
ThT Fluorescence (a.u)
50 uM
2 uM
480
490
500
510
520
530
Wavelenghth (nm)
B
6000
5000
4000
3000
2000
1000
0
ThT Fluorescence (au)
Ovalbumin
BSA
0
10
20
30
40
50
[ThT] ∝M

Fig-7

Fig-8 ThT fluorescence changes with native proteins: As in the case of Fig-7B, Panel A and Panel B here show changes in ThT fluorescence at constant protein concentrations (15 uM) but increasing ThT concentration. Both studies were carried out in phosphate buffer pH 7.4 at room temperature. Samples were excited at 444 nm and emission recorded at 495 nm. Panel A shows mostly ThT binding proteins and panel B shows mostly non-ThT binding proteins.

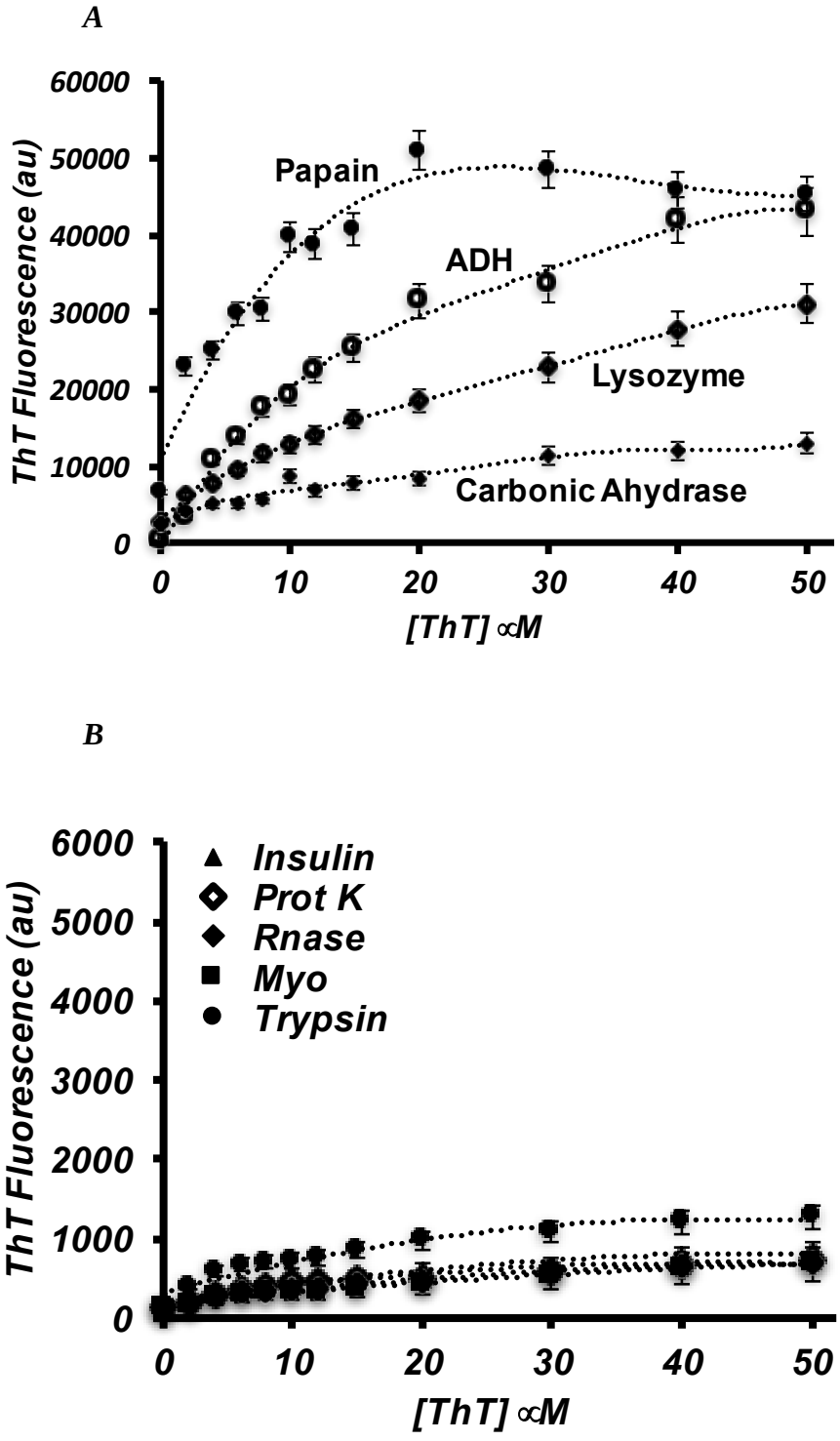
A
60000
50000
40000
30000
20000
10000
0
ThT Fluorescence (au)
Papain
ADH
Lysozyme
Carbonic Ahydrase
0
10
20
30
40
50
[ThT] ∝M
B
6000
5000
4000
3000
2000
1000
0
ThT Fluorescence (au)
Insulin
Prot K
Rnase
Myo
Trypsin
0
10
20
30
40
50
[ThT] ∝M

Fig-8

BSA in 2:1 ratio. To further the study, we analyzed the interaction of a variety of proteins with ThT. Fig-8A shows

Papain ADH and Lysozyme exhibited a significant binding to ThT with papain binding ThT in the ratio of 1:1. ADH and Lysozyme do not appear to plateau within the concentration range studied here. Interestingly, the other set of proteins insulin, proteinase K, RNase, Myoglobin and Trypsin do not exhibit significant changes in ThT emission at 495 nm even at 50 μM ThT concentration. Although trypsin and carbonic anhydrase stands out from the set of non-binders but their binding is weak and therefore, they are grouped with the non-binders. To summarize ThT does not uniformly and universally bind with all proteins some of them are avid binders some do not bind at all. The binding of ThT thus may be related to the amino acid composition and structure of the protein. It should be noted that ThT molecule by itself exhibited no change in fluorescence at all these concentrations and has been plotted as control in Fig-9.

To analyze the contribution of structure of protein on ThT-protein interaction we carried out the fluorescence experiments of all these proteins in the presence of 15.5 mM DTT and increasing ThT concentration. As shown in Fig-9. The results were again interesting; the emitted fluorescence was quite higher in the case of ovalbumin and BSA in the presence of DTT compared to in its absence (Fig-9A). Secondly, contrary to what was found in the absence of DTT, the fluorescence intensity saturated at about 15 μM of BSA showing 1:1 binding ratio under these conditions. Similarly, ovalbumin exhibited higher binding that saturated more likely at a 1:3 ratio. Control ThT only and ThT+DTT profiles were superimposable, demonstrating that the observed results were not due to a DTT effect on ThT. It is more likely the structural changes caused by disulfide disruption influences ThT interaction with proteins. Papain and lysozyme behavior also changed in the presence of DTT in that their fluorescence decreased significantly

within the group of non-interacting proteins (Fig-9B). The non-interacting proteins insulin, proteinase K, RNase, Myoglobin and Trypsin exhibited similar fluorescence changes in the absence or presence DTT (Fig-9B).

Taken together these studies show the ThT interaction with proteins is influenced by structural changes of proteins significantly.

ELISA for confirming the interaction of ThT with proteins:

To get additional support for ThT binding with the proteins, we carried out ELISA type experiments. ThT at different concentrations was placed in the wells of Nunc ELISA plates and incubated at RT overnight. Next the wells were washed with buffer and different proteins but at uniform concentration of 15 μM were placed in corresponding wells and the plate was incubated for 2 hours at RT. After incubation the plate was again washed few times and finally each well was filled with buffer. The plate was read for ThT fluorescence emission at 495 nm on a plate reader. The data has been summarized in Fig 10. The results observed in Fig-7 were reproduced. Ovalbumin again exhibited a saturation at 1:1 (protein:ThT) ratio and BSA a saturation at 2:1 ratio. Myoglobin and RNase repeated the non-ThT binding behavior under these conditions. This particular experiment was also repeated inversely in that the proteins at increasing concentrations were bound overnight to the nunc plate and then treated with uniform ThT concentration followed by incubation for 2 hours. The data showed same trend (data not shown). These studies therefore confirmed our initial inference that ThT was indeed binding to some proteins selectively while others preferred to stay away form it.

Fig-9 ThT fluorescence changes with native proteins in the presence of DTT. As in the case of Fig-7 and 8, Panel A and Panel B here show changes in ThT fluorescence at constant protein concentrations (15 uM) but increasing ThT concentration and in the presence of DTT. Both studies were carried out in phosphate buffer pH 7.4 at room temperature and 15.5 mM DTT. Samples were excited at 444 nm and emission recorded at 495 nm. Panel A shows mostly ThT binding proteins and panel B shows mostly non-ThT binding proteins

A

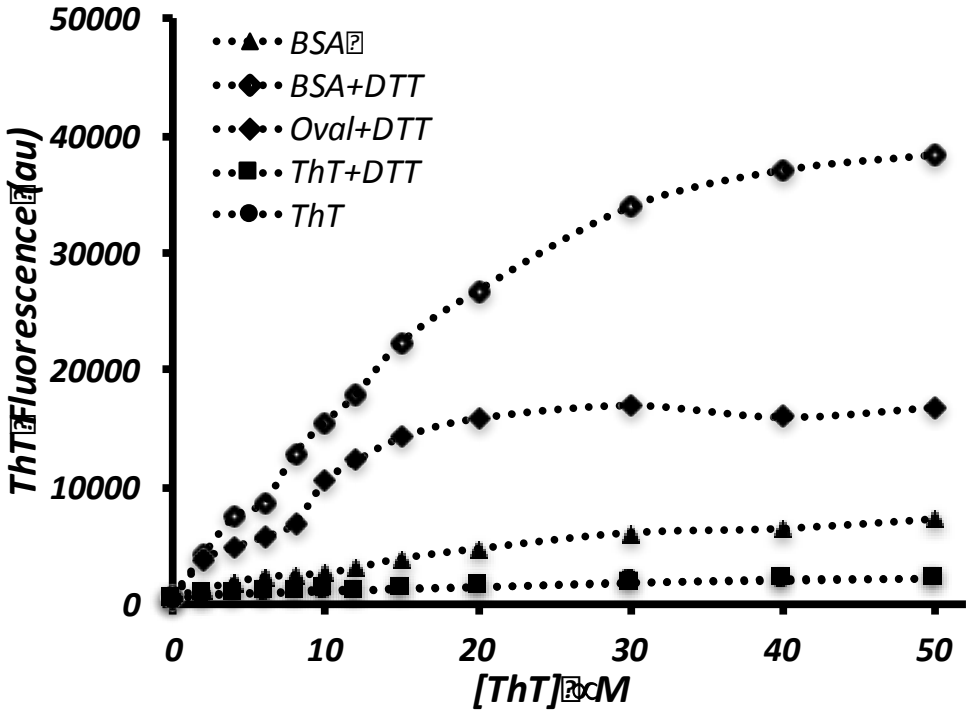
50000
40000
30000
20000
10000
0
0
10
20
30
40
50
BSA
BSA+DTT
Oval+DTT
ThT+DTT
ThT

B

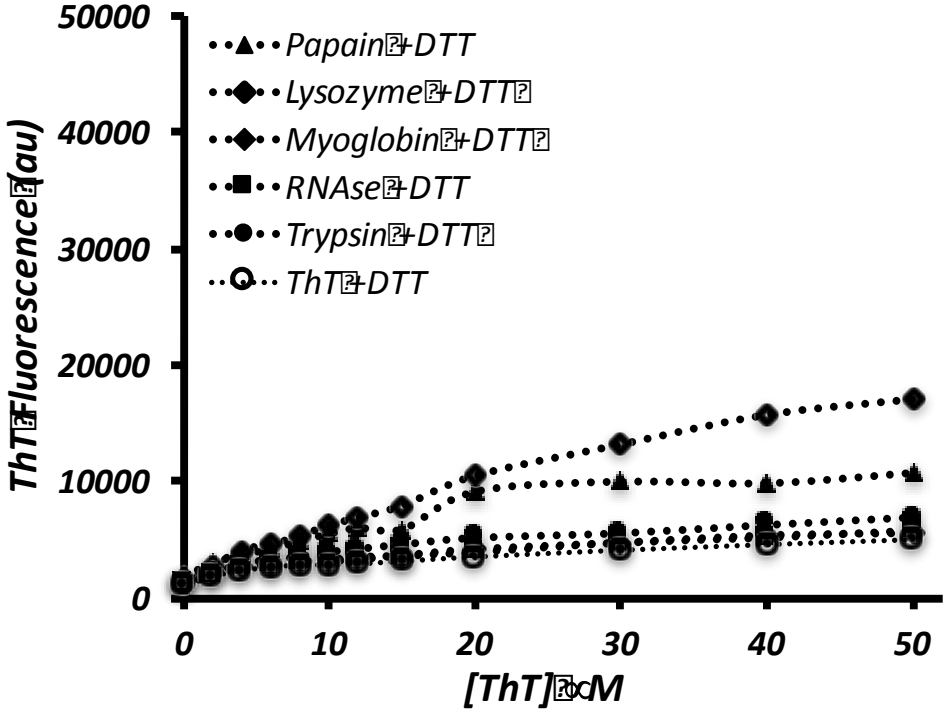
50000
40000
30000
20000
10000
0
0
10
20
30
40
50
Papain+DTT
Lysozyme+DTT
Myoglobin+DTT
RNAse+DTT
Trypsin+DTT
ThT+DTT

Fig-9

Fig -10 ELISA: figure shows binding of proteins with immobilized ThT on wells of nunc plates. ThT was incubated at increasing concentration in corresponding wells over night, washed three times next morning and incubated with protein at 15 uM concentration uniformly throughout the wells for 2 hours at room temperature. The wells were then washed with buffer and filled with 200 uL buffer and read for ThT fluorescence at 495nm. Excitation was 444 nm. ThT binding proteins again exhibited high ThT fluorescence and non-binders were found emitting around the base lines.

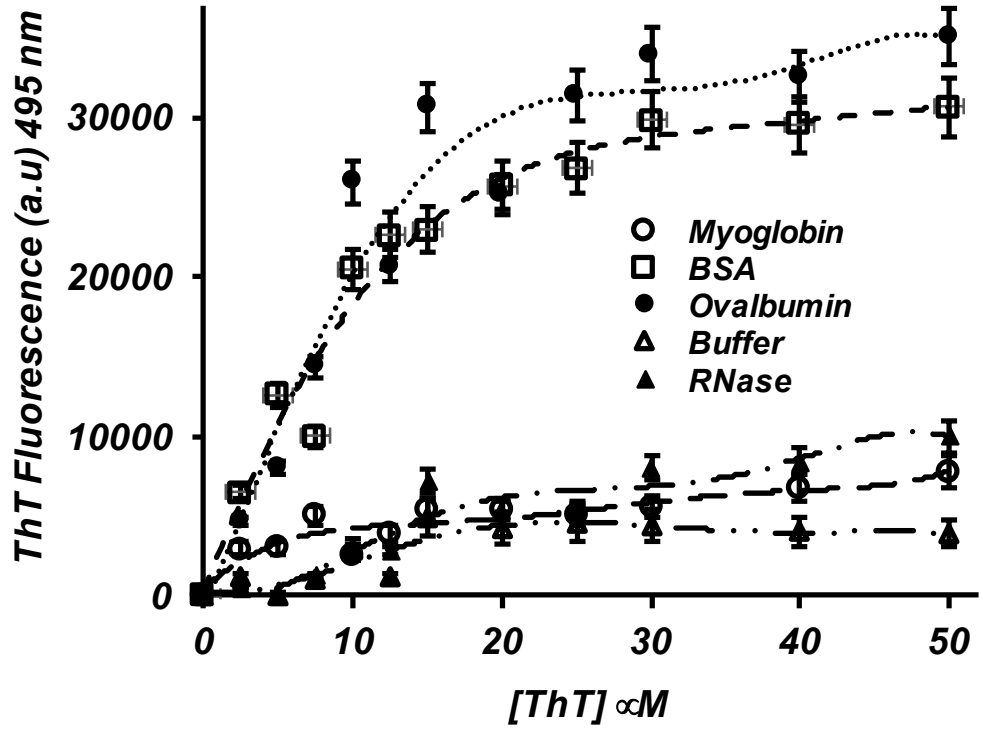
ThT Fluorescence (a.u) 495 nm
30000
20000
10000
0
0
10
20
30
40
50
[ThT] ∝M
Myoglobin
BSA
Ovalbumin
Buffer
RNase

Fig -10

Circular dichroism:

The preceding sections established that ThT was binding to a group of proteins and DTT studies indicated that this binding might be influenced by the structural changes in the protein molecule. Therefore, we designed circular dichroism experiments to monitor changes in the secondary structure of these proteins with and without the addition of ThT. Shown in Fig-11 is the far-uv CD spectra of BSA at different ThT concentrations. The CD spectrum of native untreated BSA (0.5 **μ**M) exhibits two minima around 222 nmand 209 nm. This signature profile is characteristic of proteins with predominantly α-helical secondary structure. BSA treated with 15 **μ**M ThT exhibited a loss in the signal at 222 and 209 nm indicating the loss in helical content. An increase in ThT to 50 μM lead to further decrease in the signal around these characteristic wavelengths. These experiments indicated that addition of ThT induces a structural change in BSA molecule under these conditions. The far-uv CD of myoglobin did not show any significant changes in the spectra with and without the presence of ThT. As shown in the Fig-11B the CD profiles of native and 50 μM ThT containing myoglobin samples are superimposable over each other. These results again support the selective binding of ThT to protein molecules and that ThT binding can result in the modification of the structure of protein molecules. It has been shown in many instances that he loss of structure in the proteins can reflect directly on the stability of the protein. To test this aspect we planned to carry out the thermal melts on the CD machine. BSA at 0.5 μM in 20 mM phosphate buffer ph 7.4 with or without varying concentrations of ThT was poured in a quartz cuvette and the cuvette was placed in cell holder of a CD machine. The temperature of cell was increased by peltier system at the rate of 1 °C per minute. CD signal (ellipticity was monitored) at 222 nm. The raw data was converted into fraction folded by using the protocol published by Greenfield (Greenfield, 2006a; Greenfield, 2006b). This protocol also

Fig-11 Far-UV CD profiles of Proteins: Top panel, Far-UV CD spectra of BSA at pH 7.4 in the presence of various ThT concentrations, dashed – Native BSA; solid BSA + 15 uM ThT and dotted – BSA+30 uM ThT. Bottom panel, Far-UV CD spectra of myoglobin at pH 7.4 in the presence of various ThT concentrations, Blue – Native Myoglobin only; red BSA + 15 uM ThT and purple – Myoglobin+30 uM. The protein concentration was 0.5 μM in each in 20 mM phosphate buffer pH 7.4

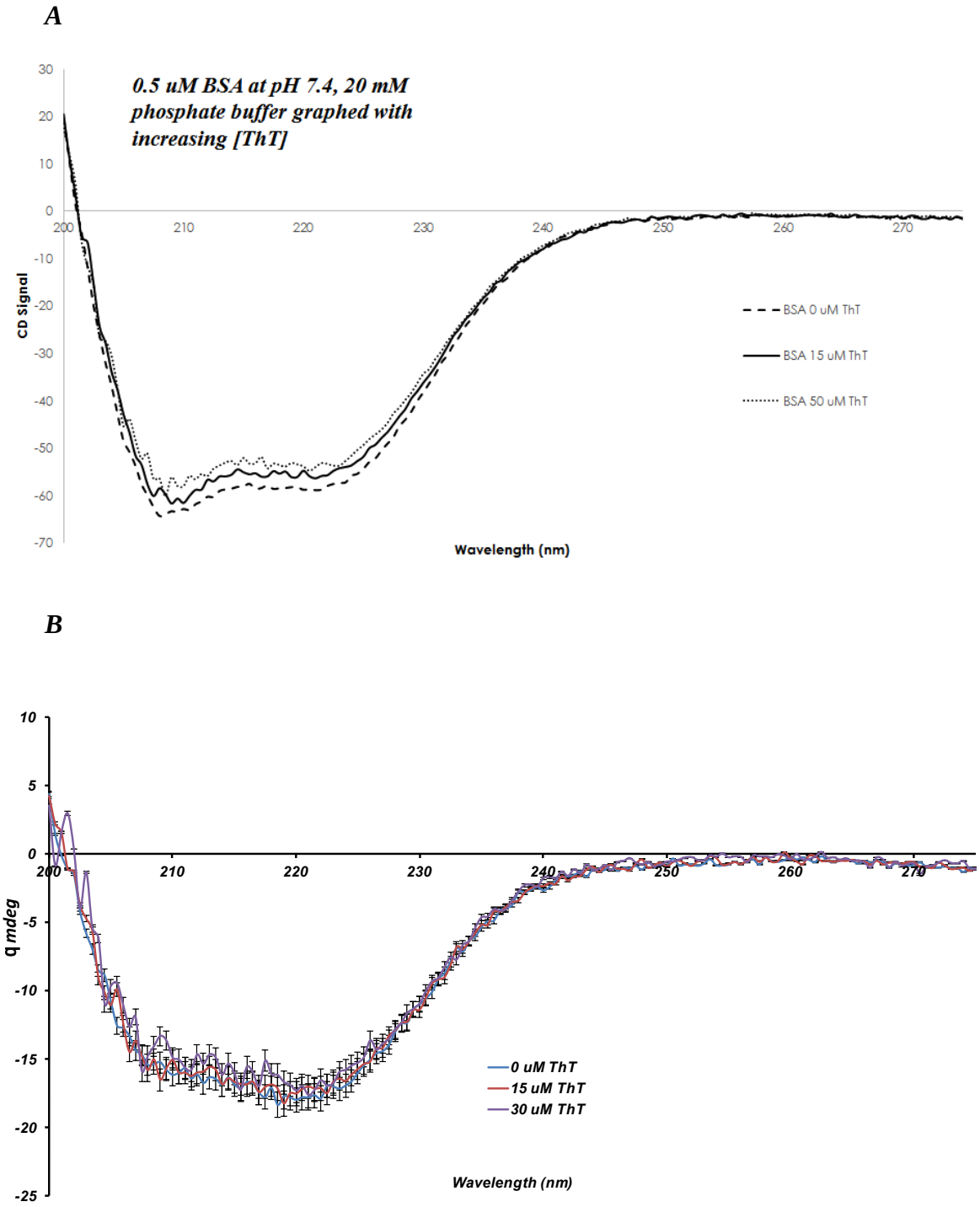
A
0.5 uM BSA at pH 7.4, 20 mM phosphate buffer graphed with increasing [ThT]
CD signal
Wavelength (nm)
BSA 0 uM ThT
BSA 15 uM ThT
BSA 50 uM ThT
B
q mdeg
Wavelength (nm)
0 uM ThT
15 uM ThT
30 uM ThT

Fig-11

Fig-12 CD changes of native proteins as a function of temperature (thermal melts): Panel A, thermal melt of BSA 1-BSA alone, 2-BSA+10 μM ThT, 3-BSA+30 μM ThT; Panel B, thermal melt of Myoglobin 1-Myoglobin alone, 2-Myoglobin +30 μM ThT. 0.5 uM protein was incubated in the presence or absence of ThT as shown in CD and temperature of the cell increased at the rate of 1 °C per minute at CD measured at 222 nm.

A

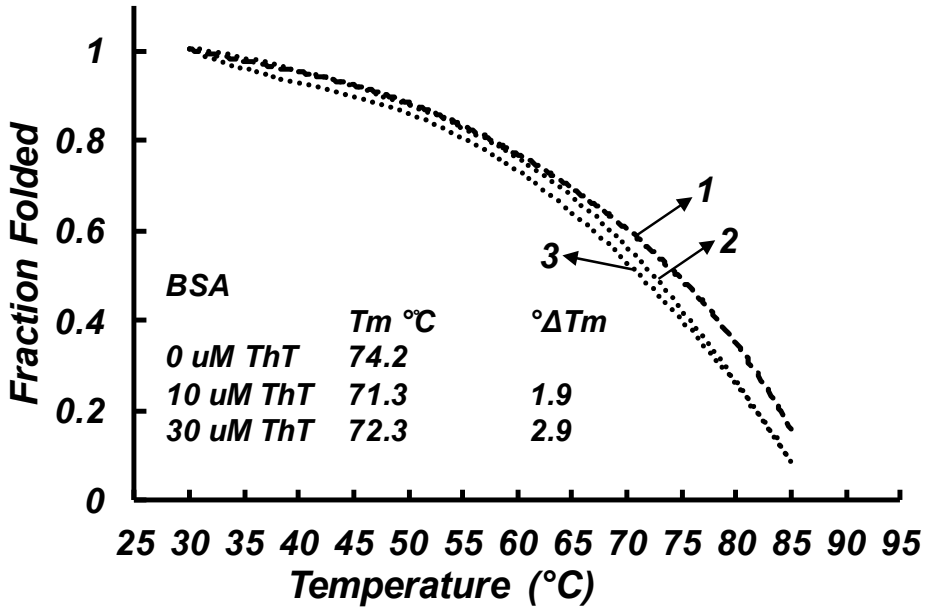
Fraction Folded
1
0.8
0.6
0.4
0.2
0
BSA
Tm ℃
°ΔTm
0 uM ThT 74.2
10 uM ThT 71.3 1.9
30 uM ThT 72.3 2.9
1
2
3
25 30 35 40 45 50 55 60 65 70 75 80 85 90 95
Temperature (°C)

B

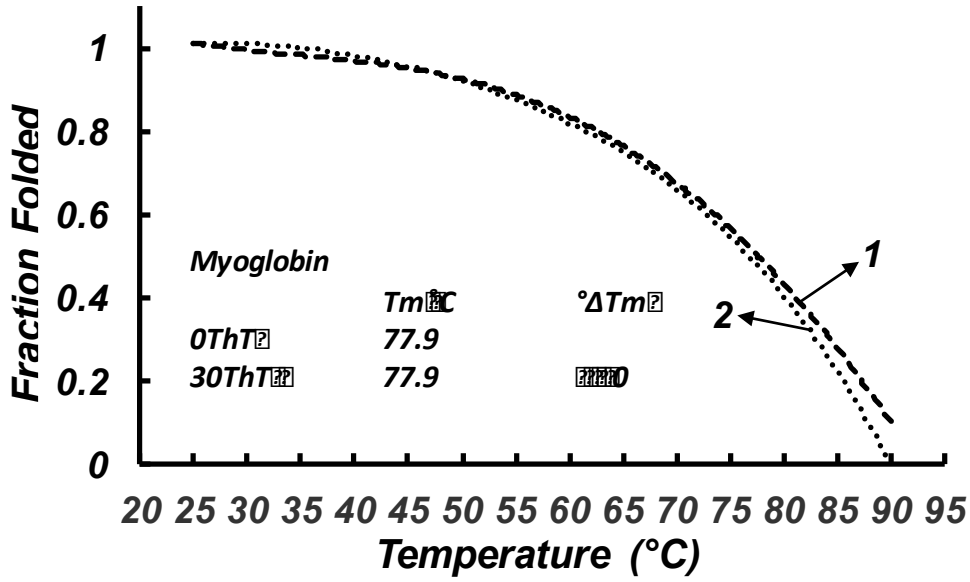
Fraction Folded
1
0.8
0.6
0.4
0.2
0
Myoglobin
Tm
°ΔTm
0ThT 77.9
30ThT 77.9
1
2
20 25 30 35 40 45 50 55 60 65 70 75 80 85 90 95
Temperature (°C)

Fig-12

provided us with the information about the melting temperature (Tm) of the protein (temperature where half the population of proteins is unfolded. As shown in the Fig-12A the Tm of BSA alone was found to be 74.2 °C. In the presence of 10 μM ThT Tm of BSA was observed to decrease to 72.3 °C and in the presence of 30 μM ThT, the Tm further decreased to 71.3 °C. These results match with the loss of secondary structure (helical content) observed in far UV CD studies upon addition of ThT. Interestingly, myoglobin the protein among the non-ThT interacting group did nto show any changes in the Tm. Melting temperature of myoglobin both in the presence and absence was observes to be 77.9 °C as shown in Fig-12B.

Thus, so far, we have confirmed ThT interacts selectively with some proteins, induces a structural change in them and that in in turn decreases the protein stability. Non-ThT interacting proteins neither observed any ThT binding nor did the presence of ThT on any detectable scale affect the stability of tehse proteins.

Effect of ThT on the aggregation propensity of BSA:

According to a seminal work by Dobson's group (Fändrich et al., 2001)any protein can form amyloid fibrils under its suitable conditions especially at high temperatures. Also, according to amyloid cascade theory (Hardy. and Selkoe., 2002; Walsh and Selkoe, 2007)proteins amyloid formation is step wise with protein unfolding ro structural modification as the first trigger factor. Keeping both of these in mind and comparing it with ThT data we summarized above, we wanted to explore if addition of ThT could influence the aggregation propensity of BSA. We used ThT assay to determine the aggregation propensity of BSA in the presence or absence of high concentrations of ThT as shown in Fig-13. BSA was incubated under the amyloid forming conditions (37 °C, pH 7.4, 600 rpm) in the presence or absence of varying concentrations of ThT (co-incubation), aliquots drawn at regular intervals and fluorescence measured. The raw

Fig-13 ThT fluorescence changes upon BSA aggregation: Panel A, Shows ThT fluorescence as a function of time during BSA amyloid formation in increasing concentrations of ThT as shown against each profile. BSA was incubated for 2 hours at 37 °C stirred at 600 rpm in 20 mM phosphate buffer pH 7.4. Panel B, shows the normalized data ((F0-F)/[ThT]) where F0 is fluorescence in the absence of ThT at 0 time of incubation, F is fluorescence at any time of incubation either in the presence or absence of ThT.

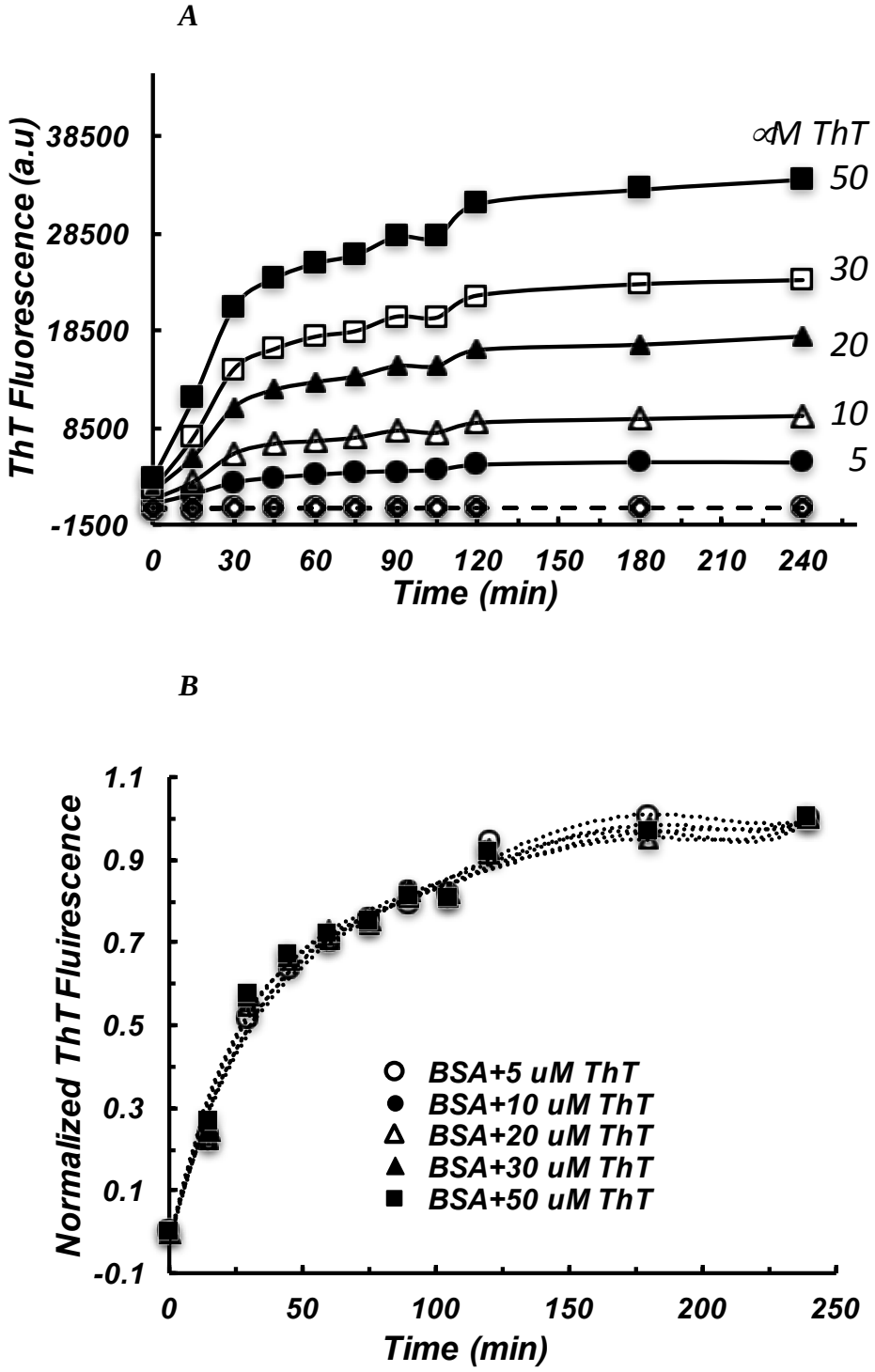
A
ThT Fluorescence (a.u)
38500
28500
18500
8500
-1500
0
30
60
90
120
150
180
210
240
Time (min)
∝M ThT
50
30
20
10
5
B
Normalized ThT Fluirescence
1.1
0.9
0.7
0.5
0.3
0.1
-0.1
0
50
100
150
200
250
Time (min)
BSA+5 uM ThT
BSA+10 uM ThT
BSA+20 uM ThT
BSA+30 uM ThT
BSA+50 uM ThT

Fig-13

fluorescence data (Fig-13A) shows no increase in ThT fluorescence over 4hours of incubation. This does not mean there are no fibrils formed under these conditions but that with no fibril detection probe (ThT in this case) they cannot be detected. The fluorescence intensity as expected exhibited as increased with the time of incubation in the presence of ThT (5- 50 μM). The ThT intensity differences between profiles is masked by increasing ThT concentration and any change in the rate of amyloidosis cannot be observed. Therefore, the data was corrected for the contribution of ThT concentration by diving the net fluorescence by amount of ThT present in each case. The resulting profiles (Fig-13B) appear to be closely following each other towards the aggregation process. There is a subtle change in the propensity thought, for example, ThT in the presence of 50 μM ThT exhibits a 4% decrease in lag time compared with the 5 μM ThT. The changes are linear but the effect is not significant. We repeated these experiments by incubating BSA under the similar conditions but without any ThT. Aliquots were collected at desired time and then 50 μM ThT was added to one part before recording the fluorescence. The resulting profile was not significantly different. To other part 5 μM ThT was added and it again produced the similar profile as was observed in the case where ThT was co-incubated.

These experiments in summary showed that ThT binding does not have a significant observable effect on amyloid genesis of BSA under these conditions.

Crystallography studies of ThT binding to BSA:

BSA was crystallized according to the protocols published previously (Majorek et al., 2012) by hanging drop method. BSA at final concentration of 10 mg/mL in the tank buffer containing PEG 5000 was placed in as a drop on the cover slip and sealed in the well of a=the crystallization plate. The plate was incubated at 20 °C. After three weeks (21 days) crystals were visible and started to grow big. The crystals looked needle-like and appeared flat and unidirectional. (Fig-

14a, b) The needles were 73 μm wide at some places. After consultations with crystallographers it was suggested that these crystals might not diffract well. So, we modified the protocol and set hanging drops of BSA 10 mg/mL final concentration in PEG 3350, pH 6.25 Tris-HCl. and incubated them at 16 °C. Again, after three weeks the crystals were visible. The crystals appeared big this time with a width of about 140 μm (Fig-14c, d). The crystals were sent for diffraction to Chicago accelerator and diffracted at 4Å. This diffraction was supposed to be not sensitive enough to provide the details of binding of a small molecule like ThT.

From these studies, we were left with just one option of finding the probable binding site of ThT on BSA and that was molecular docking. We used auto dock software to float the ThT molecule on BSA environment and locate the lowest energy binding site on BSA.

Fig 14 Crystallography of BSA molecule: BSA was crystallized using hanging drop method. Reservoir buffer with 20% PEG 3350 w/v and 0.2 M calcium acetate in 0.1 M Tris HCl buffer, pH 6.5 was placed in the reservoir wells. BSA samples were made by mixing 1:1 with the reservoir buffer in a final volume of 10 µL. The stocks were made such that final concentrations in the drop was 20 mg/mL (300 µM) BSA + 0 µM ThT (a); or 20 mg/mL (300 µM) BSA + 30 µM ThT (b). Three drops of each sample were placed on siliconized coverslip. Coverslips were capped on the wells and sealed with vacuum grease. The plate was incubated in a constant 20 °C incubator and crystal growth monitored for three weeks. Crystals shown in (c) and (d) correspond to 20 mg/mL BSA + 0 µM ThT and 30 mg/mL BSA + 30 µM ThT respectively. Both (c) and (d) used PEG 3350 in Tris-HCl buffer at pH 6.25 and was incubated at 20 C. Crystals grew in 3 weeks.

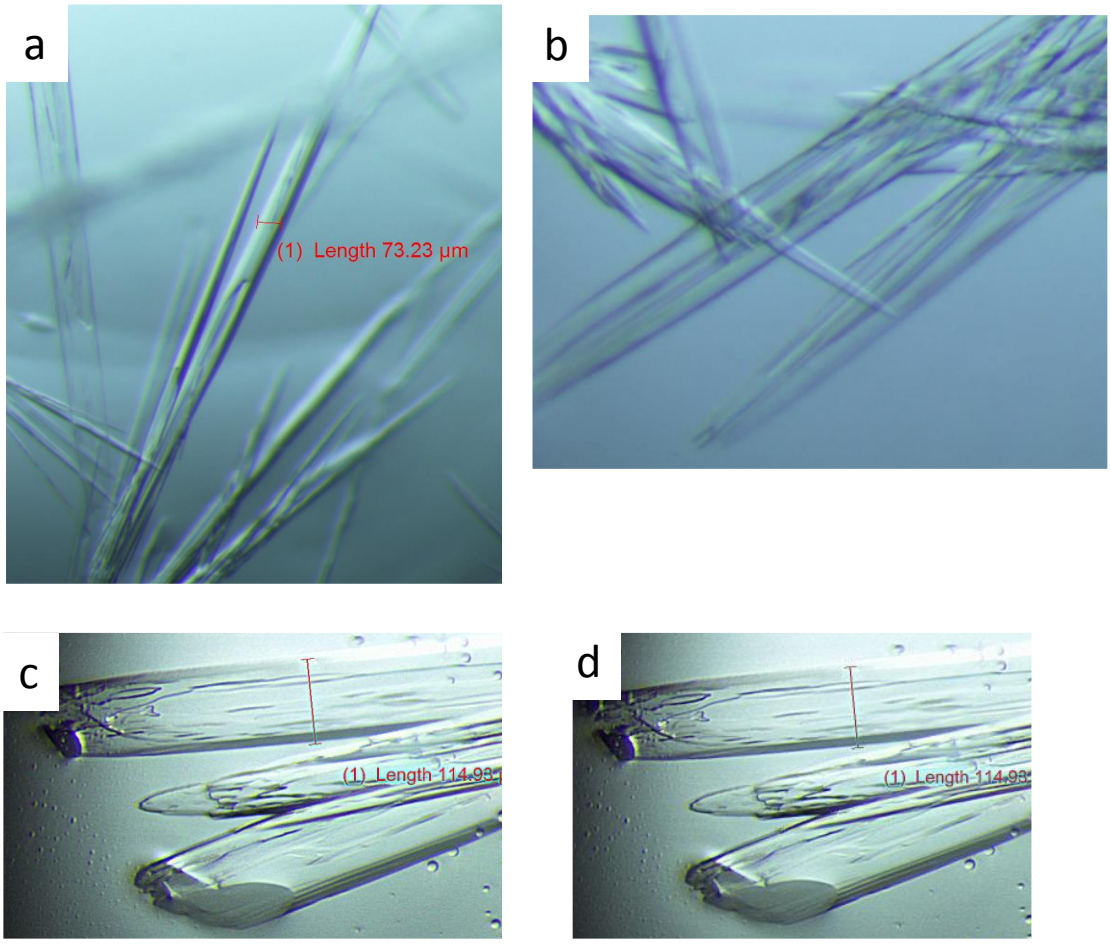

Fig 14

Using computational simulations software AutoDock to locate ThT binding site

Blind docking simulations were carried out with Auto Dock 4.2. We used AUTODOCK 4.2 in different ways to validate our results obtained from this method. First, we ran a known BSA moecuel with a known lgand whose location ahd been solved both by AUTODOCK 4.2 and crystal structure. After gaining confidence in parameter setting in this exercise we ran AUTODOCK 4.2 on full length BSA molecule and located the binding site corresponding to the lowest ΔG. Next we used the dimer and located the binding site with lowest energy. The BSA molecule was further fragmented computationally and AUTODOCK 4.2 was run on each of the fragment. The redundant sites with the lowest energy were considered most potential binding site (see table 4).

Repeated conformation 'hits' between simulations were noted and used to reinforce confidence in binding sites, with lowest binding site energy from these 'hits' were totaled in order to calculate a total **Δ** G for that binding site. The corresponding docking summary for the complexes are listed on Table 4 and suggests that a preferential binding site exists between amino acids (AA) 1 to 300 of BSA (Fig. 23) with a total **Δ** G of -131.38 kcal/mol, with a secondary site between AA 500-600 with a total **Δ** G of -77.31 kcal/mol. These calculations were carried out with ThT as a flexible ligand, while the protein conformation was constrained. All hydrogens were added to the structures simultaneously, while Gasteiger charges were assigned to the protein and a Larmarkian genetic algorithm was used to calculate binding sites.

The zoomed in ThT binding site on BSA (with ThT structure) has been shown in Fig-15 and the location of binding site with respect to the whole BSA molecule has been shown in Fig-16.

Based on the simulation studies it was clear that ThT binds in the aromatic rich region. In order to derive a pattern that could discriminate between the properties of ThT binding in the case of ThT-binding and ThT-non binding proteins, we populated various parameter of these different proteins using available data and our own calculations. For example we found % helical and beta sheet content from published PDB structures. We calculated the number of aromatic and hydrophobic residues using online tools. Once collected, we plotted each of these parameters from each protein with the changes in ThT observed for the corresponding protein. The data is presented in Fig-17 and 18. If we look closely the data does nto exhibit a trend in any of the cases shown. For example, BSA with more hydrophobic content exhibits lower ThT signal and and insulin with highest % hydrophobic content exhibits lowest ThT signal. Agian for % aromaticity although ovalbumin and BSA follow the trend but lysozyme, Prot. K or insulin with higher content exhibit lower ThT binding.

Table 4 Summarizes Autodock parameters

	AutoDock Energy Scores						
	Fragments	1-300 fragment (-DG)	300-400 fragment (-DG)	400-500 fragment (-DG)	500-600 fragment (-DG)		
RMSD +	Redundant Scoring	19	1	3	10		
RMSD -	Non-Redundant Score	11	1	3	3		
	Energy (kcal/mol)	-7.62	-5.42	-6.13	-7.24		
	Total ΔG (kcal/mol)	-131.38	-5.42	-18.89	-77.31		
	Grid coordinates for running AutoDock						
	Coordinates	1-300	300-400	400-500	500-600		
Center	x	36.953	27.616	43.029	65.244		
	y	28.191	22.997	14.499	12.676		
	z	27.436	57.13	51.756	57.676		
	spacing	0.497222222	0.497222222	0.497222222	0.375		
	x Grid Points	126	126	78	94		
	y Grid Points	106	80	94	94		
	Z Grid Points	118	72	64	82		
	Coordinates	50-150	250-350	350-450	450-550		
Center	x	45.868	17.226	28.55	48.498		
	y	28.191	32.652	17.5	12.168		
	z	23.269	39.844	56.624	54.34		
	spacing	0.497222222	0.497222222	0.497222222	0.497222222		
	x Grid Points	92	86	122	104		
	y Grid Points	106	88	82	84		
	Z Grid Points	84	82	66	72		

.

Fig-15 ThT binding site (zoomed in) in BSA based on AutoDock data. Result of AutoDock simulation showing binding pocket of ThT in fragment 1-300 of BSA. Residues closest to ThT labeled with amino acid structure shown superimposed on secondary structure of BSA.

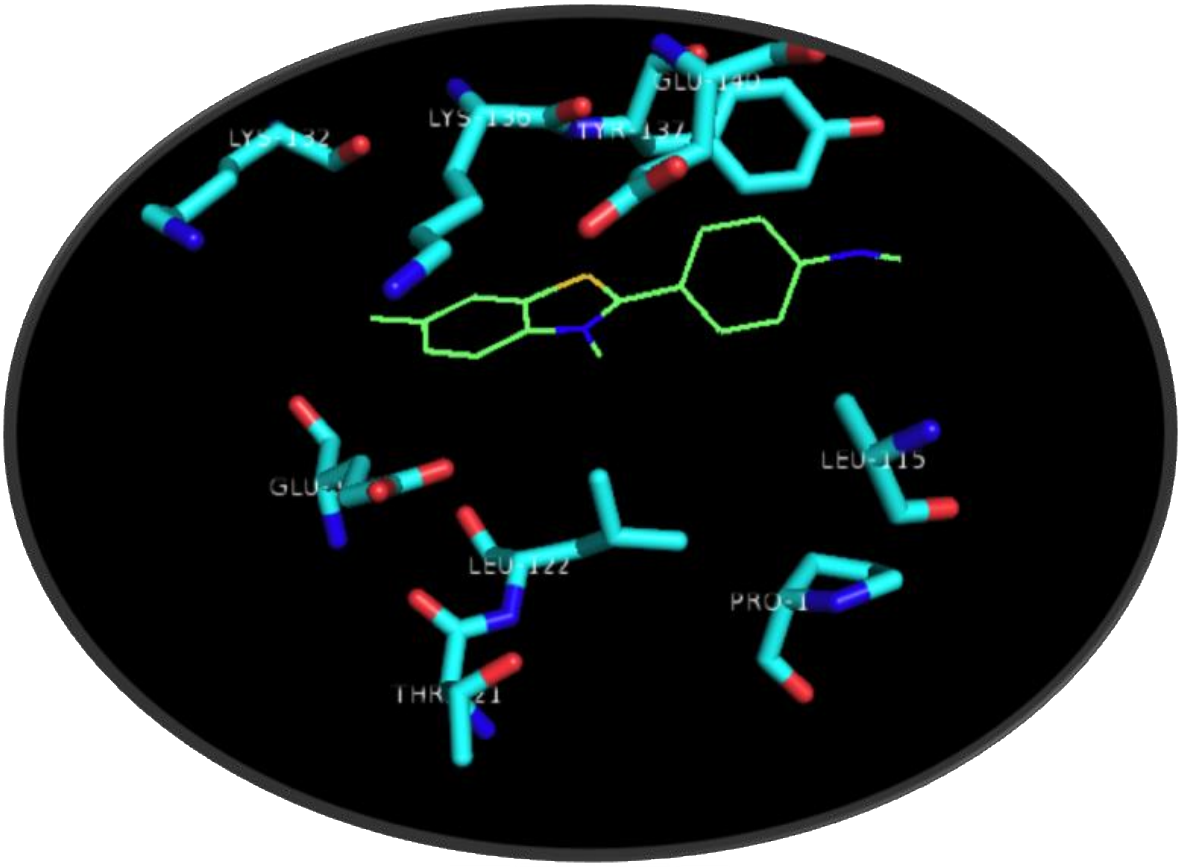
LYS-132
LYS-135
TYR-137
GLU-140
GLU-1
LEU-115
LEU-122
PRO-1
THR-121

Fig-15

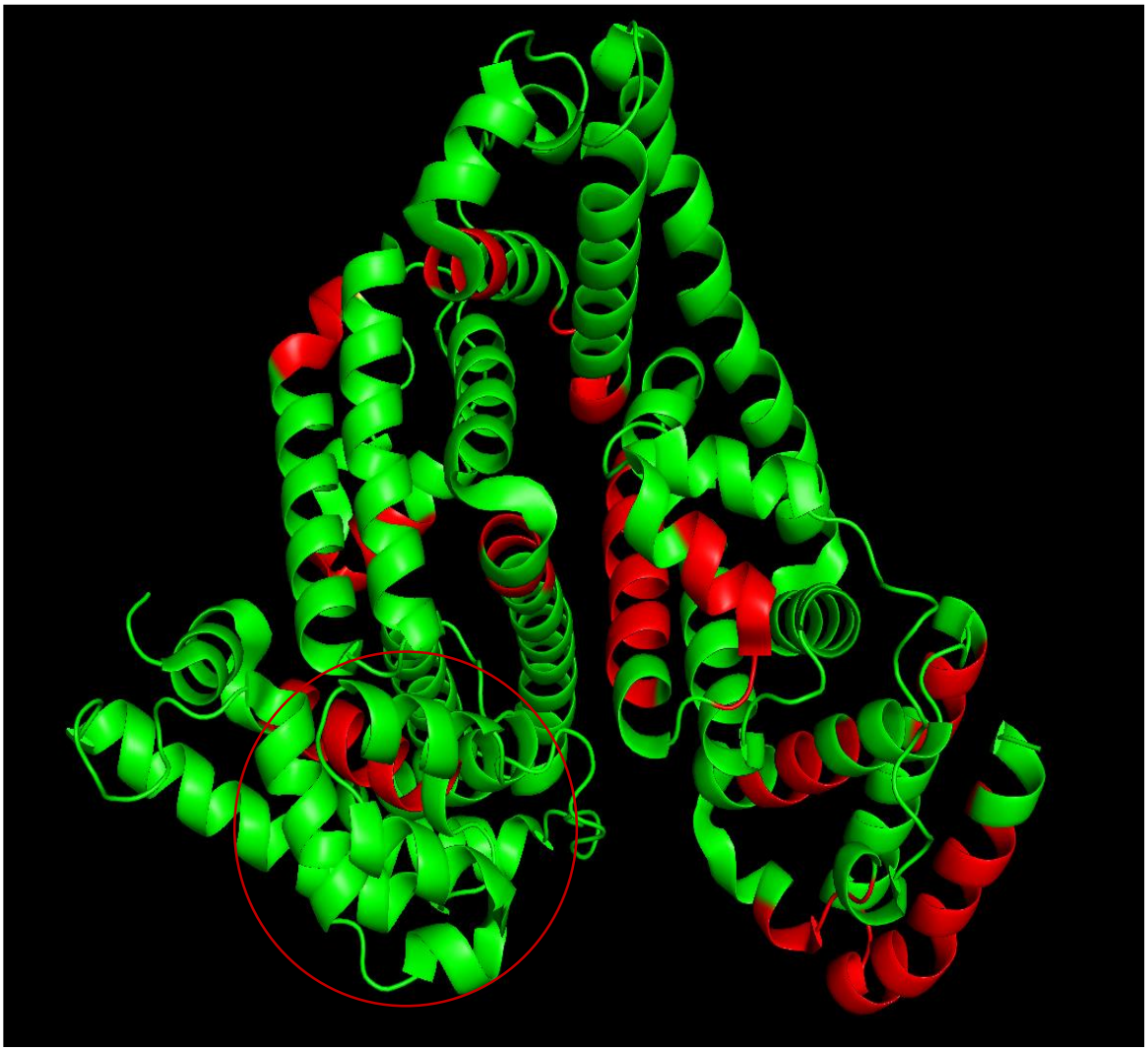

Fig-16 ThT binding site with respect to full length BSA molecule based on AutoDock data.

Fig-17 Plot of ThT fluorescence vs % beta sheet and alpha helix content of different proteins. The parameters were either obtained from PDB files or calculated using online tools.

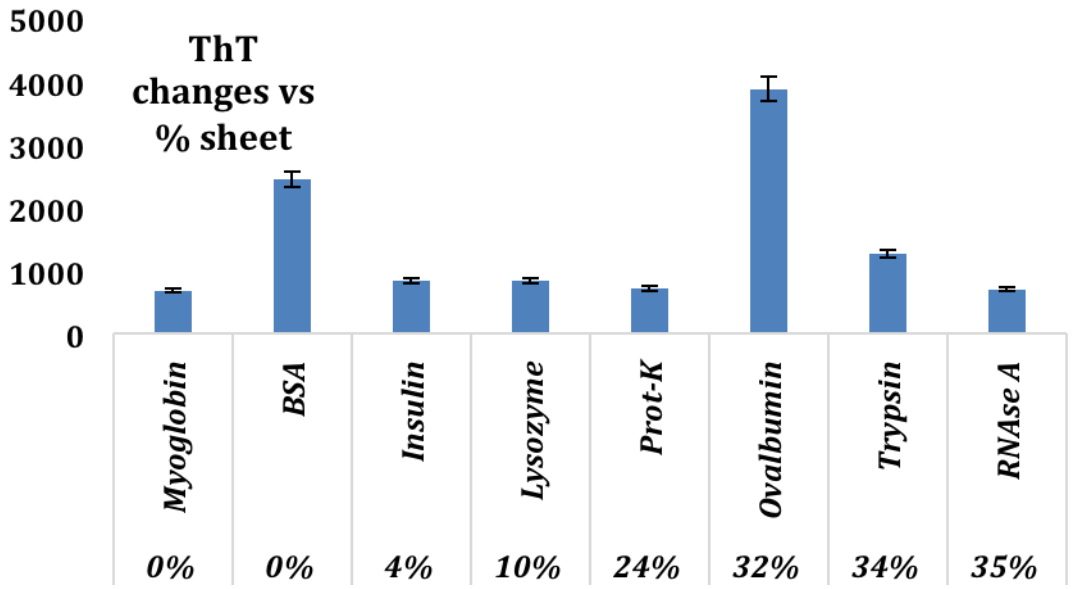
ThT changes vs % sheet
5000
4000
3000
2000
1000
0
Myoglobin
BSA
Insulin
Lysozyme
Prot-K
Ovalbumin
Trypsin
RNAse A
0%
0%
4%
10%
24%
32%
34%
35%

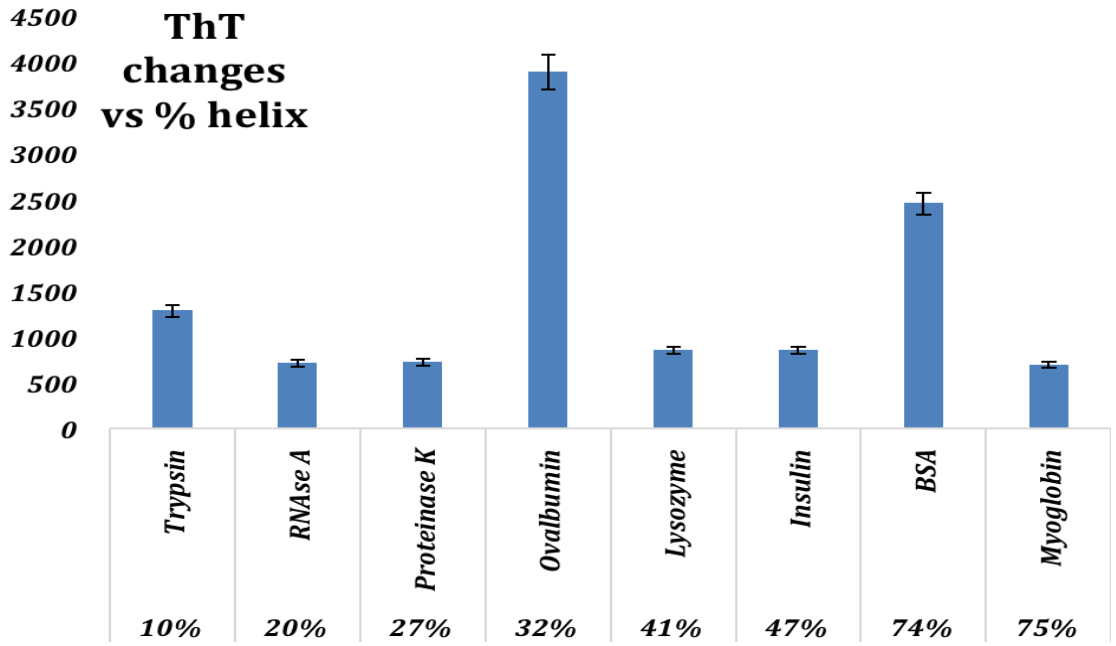
ThT changes vs % helix
4500
4000
3500
3000
2500
2000
1500
1000
500
0
Trypsin
RNAse A
Proteinase K
Ovalbumin
Lysozyme
Insulin
BSA
Myoglobin
10%
20%
27%
32%
41%
47%
74%
75%

Fig-17

Fig-18 Plot of ThT fluorescence vs % aromaticity and hydrophobicity content of different proteins. The parameters were either obtained from PDB files or calculated using online tools.

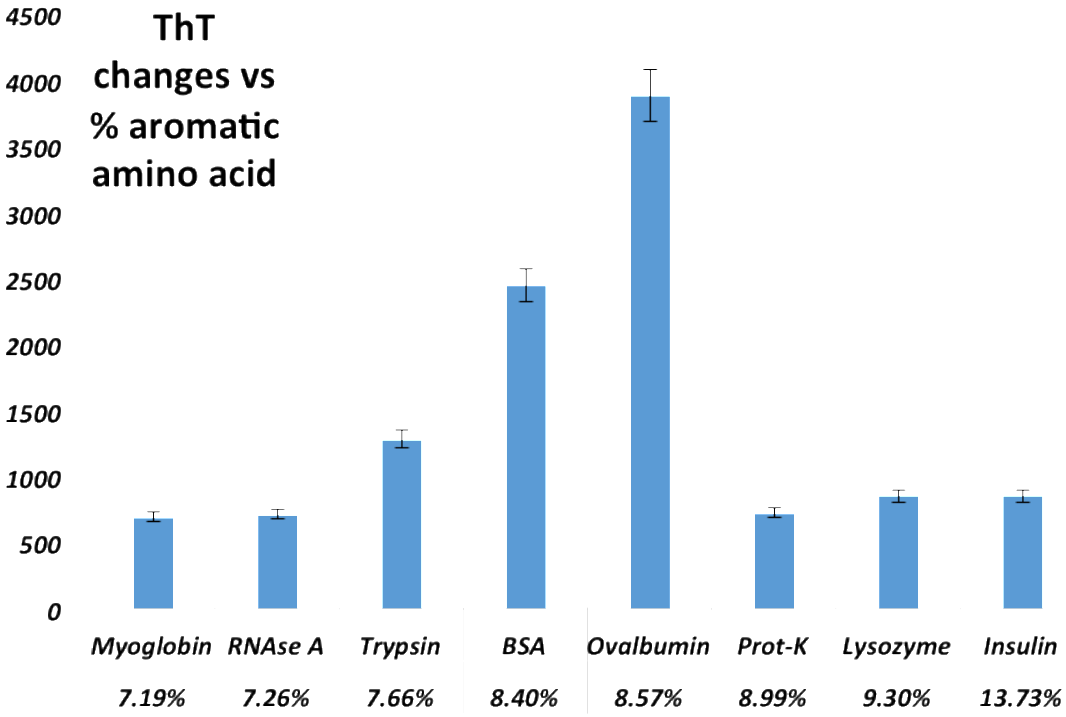
ThT changes vs % aromatic amino acid
4500
4000
3500
3000
2500
2000
1500
1000
500
0
Myoglobin
RNAse A
Trypsin
BSA
Ovalbumin
Prot-K
Lysozyme
Insulin
7.19%
7.26%
7.66%
8.40%
8.57%
8.99%
9.30%
13.73%

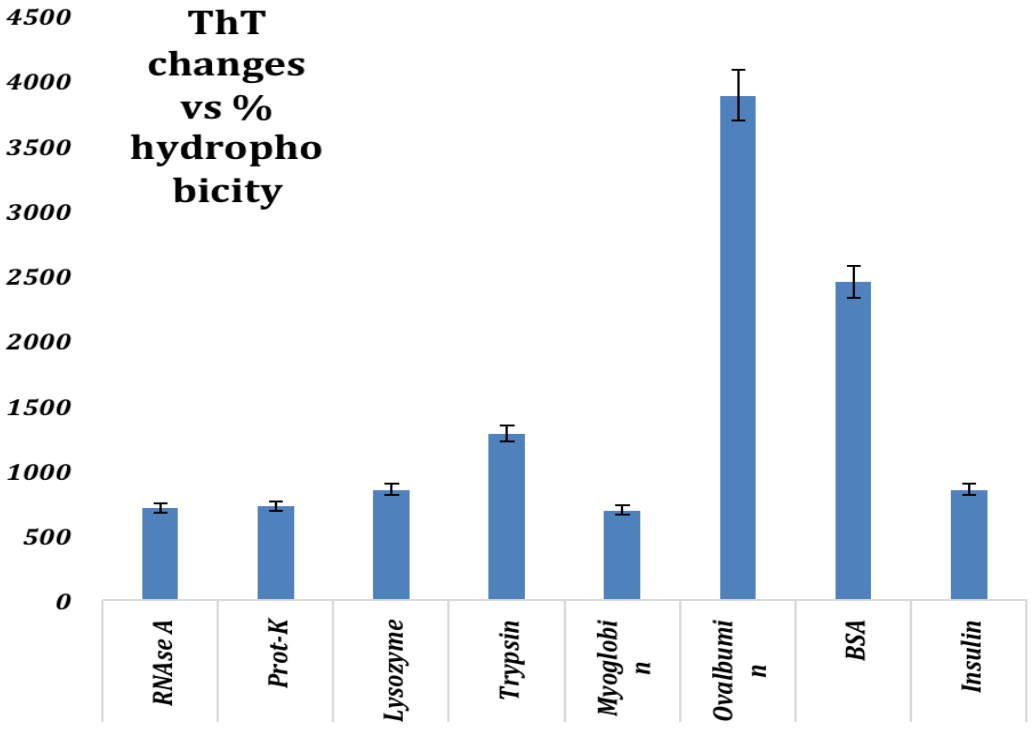
ThT changes vs % hydrophobicity
4500
4000
3500
3000
2500
2000
1500
1000
500
0
RNAse A
Prot-K
Lysozyme
Trypsin
Myoglobin
Ovalbumin
BSA
Insulin

Fig-18

Discussion:

The usefulness of ThT and the extent of information it has provided thus far in the field of amyloid research are mind-boggling (Harel et al., 2008; Krebs et al., 2005; LeVine, 1995; Naiki et al., 1989; Sulatskaya et al., 2010; Wu et al., 2008; Wu et al., 2009). ThT is a dynamic molecule that works in different pH, is not affected by metal ions and these properties make it far more superior than congo-red the traditional detection dye for amyloid (Khurana et al., 2001). So much was the influence of congo-red in the amyloid field that these diseases were initially termed "congo-files" and the patients sometimes were injected with congo-red to find amyloid (Puchtler et al., 1962; Shikama et al., 2010). The sample is highly sensitive to the thickness of the amyloid film and needs good expertise in sample preparation. The use of cross-polarized light in the congo-red assay is another requirement that decreases the degree of easiness in its use and makes the technique less popular (Kim et al., 2003).

Although EM is an easier technique, the grid preparation being commercially and economically available, the technique still is challenged in the sense that it provides the snap shorts in terms of mechanism. The technique never the less is highly sensitive on modern high magnification machines and can provide the atomic details in the fibrils a feat only possible with this technique (Jime´nez et al., 2002). X-ray diffraction again is limited in providing information about the cross beta sheet structure of the fibril. This is mainly due to the repetitive arrangement and nature of constituent molecules in the fibril but also to the fact that diffraction might not occur within a resolution on Å scale (Eanes and Glenner, 1968). The scattering of X-ray can also not provide more information about the atomic details since wide-angle scattering is very weak on normal X-ray machines and the sample stability is compromised in high beam synchrotron

facilities. Sample preparation is another technique that needs good expertize before a scientist can proceed in this direction.

During recent times and especially in the last decade investigators have tried various other fluorescent molecules namely ANS (Ahmad et al., 2005), Bis-ANS, Thioflavin-S, and as far distinct as rheology methods but ThT has been, colloquially mentioning, “irreplaceable” in terms of its ease of application, sensitivity and universality in its use with different proteins and peptides(Ahmad, 2010; Biancalana et al., 2008).

In the present work, we initially focused on detecting the BSA fibrils with ThT for an entirely different project but were quite surprised to see the native protein binding ThT during the technique standardization process in the lab. This initial finding led us to explore in this direction and analyze the range of ThT concentrations with BSA initially. The results showed us that binding was specific and each BSA appeared to bind two molecules of ThT. The process was reproducible at different concentrations of BSA. At this stage, it was rational to test its ortholog ovalbumin and the getting similar results confirmed it was not an isolated process. We therefore tried a set of proteins that we could easily find available. It soon turned out that among this set, ThT, preferentially bound to certain proteins and others it did not. The efficiency of binding also seemed to differ from protein to protein. Since BSA has free SH- group (Majorek et al., 2012) the first guess was that it is either binding to SH- group or it is affecting the fluorescence properties of ThT itself. ThT in the presence and absence of DTT did not show any changes in the fluorescence of emission and increase in fluorescence in the case of DTT treated BSA indicated neither of the assumptions was correct. In addition, some of the ThT-binders (lysozyme) in the absence of DTT changed to non-binders in the presence of DTT. These factors explained that it was more than the solvent or SH- interference going on. And since there are

many instances now available where ThT has been shown to bind non-fibrilar states, it seemed more reasonable that ThT was binding to the protein itself. The increase or decrease in fluorescence in the presence of DTT indicated that ThT under these conditions was either able to make efficient binding or was prevented form such binding, respectively, due to the changes in the structure of the molecule under the influence of DTT. Yet we felt the need of establishing ThT binding by another method and in this case we designed an EISA based immobilization of one component followed by monitoring the attachment of another component to see the extent of binding. The ELISA results were at par with fluorescence results and ELISA was again able to discriminate the ThT binders form no-binders. These results thus established beyond any degree of ambiguity that ThT was selectively binding to some proteins in non-fibrilar state or native state

Now that binding was happening, we could use some other biophysical methods to explore the consequences of such binding and any of the structural changes happening. We therefore used CD to monitor if any structural changes were taking place (Greenfield, 2006a; Uversky and Permyakov, 2007). Far-UV CD scans of BSA in the presence of ThT exhibited small but gradual changes as a function of ThT concentration. While for a non-binder like myoglobin, these changes were not observed setting apart the binders and non-binders in yet another parameter. The binding of ligands is often associated with the change in the stability of proteins. We therefore wanted to see the effect of ThT on the thermal stability of these binding proteins and use the non-binders as controls. The CD melts we performed showed in case of the ThT-binding protein the Tm decreased by ~3 °C in the presence of 30 uM ThT. On the other hand, observation of no change in the Tm for myoglobin in the presence and absence of ThT

increased our confidence in the data and the process. This also gave us confidence to further explore the exact binding site of ThT at least in the case of BSA.

We chose to do that by crystallography and were fortunate enough to get the crystals growing in the first few tries. But the crystals turned out to be needle like, flat and unidirectional and were not expected to diffract well. Further screening for temperature and pH lead us to get better thicker crystals but those crystals diffracted only up to 4 Å which was not sensitive enough data set to provide us any information at the level of ThT. In its absence, we resorted to use the computational molecular dynamic software AutoDock 4.2 to locate the binding site (Crippen et al., 2010). We tried to get robustness and confidence in out AutoDock analysis by using a set of permutations and combinations and chose to select only the redundant candidates with lowest binding energy as possible binding site for ThT. These data suggested that most probable binding site of ThT is between 1-300 residues and in a highly aromatic rich region. The most surprising observation in this simulation was that the binding sites of ThT were closer to the amyloid prone nucleating sites of BSA determined by the zipperDB prediction software as shown on right side here.

With this conclusion, we further proceeded to see if the presence or absence of aromaticity is the discriminating parameter between Tht-Binders and non-binders. The analysis on this direction was not that straight forward while the ThT binding of BSA and ovalbumin

aligned with such this binding pattern others did not. Analysis of other parameters with respect to ThT-protein binding like, hydrophobicity, helicity and others also did not provide us with a clear pattern or ability of prediction.

Based on the data presented here, this study had added to our knowledge about the aspects and diversity of ThT binding selectively to some proteins.

Conclusion:

ThT fluorescence assay has provided a wealth of information about amyloid dynamics and kinetics. In this work, we report that besides amyloid, ThT can bind to native proteins too. We established this through the ThT fluorescence changes with each protein and confirmed the data with ELISA type immobilized assay and fluorescence quenching. Based on these assays the protein population fell in two categories viz., 1) ThT-binders and 2) ThT-non-binders. Among the ThT binding proteins ThT caused change in the secondary structure and decreased their stability but did not influence their propensity to amyloidosis significantly. This property of ThT could be availed as a potential drug like activity against amyloid. Modification of ThT SAR will get more ThT like anti-amyloid molecules.

Although crystallization did not work, the simulation data located the binding site in the 1-300 residue of BSA. Surprisingly, the other binding sites laid close to the proposed nucleation fragments of BSA fibrillation. Further, analysis showed there was no structural or compositional predictor that aligned with the observed ThT binding or non-binding property of proteins. In conclusion, thus it could be stated that ThT binding to the proteins or amino acids is dependent on availability or creation of a unique aromatic rich site that can accommodate ThT effectively. And this work thus establishes that ThT can selectively bind to some proteins.

References:

Abraham, J., and Mathew, B. (2014). Synergic Effects of Anticancer Drugs to Bovine Serum Albumin: A Spectroscopic Investigation. Res J Recent Sci *3*, 157-162.

Acebrón, S.P., Fernández-Sáiz, V., Taneva, S.G., Moro, F., and Muga, A. (2008). DnaJ Recruits DnaK to Protein Aggregates. J. Biol. Chem. *283*, 1381-1390.

Ahmad, A., Stratton, C.M., Scemama, J.L., and Muzaffar, M. (2016). Effect of Ca(2+) on Aß40 fibrillation is characteristically different. Int J Biol Macromol *89*, 297-304.

Ahmad, B., Khan, M.K., Haq, S.K., and Khan, R.H. (2004a). Intermediate formation at lower urea concentration in 'B' isomer of human serum albumin: a case study using domain specific ligands. Biochem Biophys Res Commun *314*, 166-173.

Ahmad, A. (2010). DnaK/DnaJ/GrpE of Hsp70 system have differing effects on α-synuclein fibrillation involved in Parkinson's disease. Inter J Biol Macromol *46*, 275-279.

Ahmad, A., Akhtar, M.S., and Bhakuni, V. (2001). Monovalent cation-induced conformational change in glucose oxidase leading to stabilization of the enzyme. Biochemistry *40*, 1945-1955.

Ahmad, A., Millett, I.S., Doniach, S., Uversky, V.N., and Fink, A.L. (2004b). Stimulation of insulin fibrillation by urea-induced intermediates. J Biol Chem *279*, 14999-5013.

Ahmad, A., Millett, I.S., Doniach, S., Uversky, V.N., and Fink, A.L. (2003). Partially folded intermediates in insulin fibrillation. Biochemistry *42*, 11404-16.

Ahmad, A., Muzaffar, M., and Ingram, V.M. (2009). Ca^{2+}, within the physiological concentrations, selectively accelerates Aß42 fibril formation and not Aß40 in vitro. Biochim Biophys Acta *1794*, 1536-1547.

Ahmad, A., Uversky, V.N., Hong, D., and Fink, A.L. (2005). Early events in the fibrillation of monomeric insulin. J Biol Chem *280*, 42669-42675.

Ahmad, A., Burns, C.S., Fink, A.L., and Uversky, V.N. (2012). Peculiarities of Copper Binding to alpha-synuclein. J Biomol Struct Dyn *29*, 825-842.

Al-Lohedan, H.A., and Sajih, A.M. (2013). Sulfadiazine binds and unfolds bovine serum albumin: an in vitro study. Mol Biol Rep *40*, 6081-6090.

Ashburn, T.T., Han, H., McGuinness, B.F., and Lansbury, P.T.J. (1996). Amyloid probes based on Congo Red distinguish between fibrils comprising different peptides. Chem Biol *3*, 351-358.

Astbury, W.T., Dickinson, S., and Bailey, K. (1935). The X-ray interpretation of denaturation and the structure of the seed globulins. Biochemical Journal *29*, 2351-2360.

Axelsson, I. (1978). Characterization of proteins and other macromolecules by agarose gel chromatography. J Chromatog A *152*, 21.

Bennhold, H. (1922). Eine spezifische Amyloidfarbung mit Kongorot. Munchen Med Wochenschr *69*, 1537-1538.

Bhattacharya, M., Jain, N., and Mukhopadhyay, S. (2011). Insights into the mechanism of aggregation and fibril formation from bovine serum albumin. J Phys Chem B *115*, 4195-4205.

Biancalana, M., and Koide, S. (2010). Molecular mechanism of Thioflavin-T binding to amyloid fibrils. Biochim Biophys Acta *1804*, 1405-1412.

Biancalana, M., Makabe, K., Koide, A., and Koide, S. (2008). Molecular mechanism of thioflavin-T binding to the surface of beta-rich peptide self-assemblies. J Mol Biol *385*, 1052-1063.

Brenner, D.A., Buck, M., Feitelberg, S.P., and Chojkier, M. (1990). Tumor necrosis factor- α inhibits albumin gene expression in a murine model of cachexia. J Clin Invest *85*, 248-255.

Carter, D.C., and Ho, J.X. (1994). Structure of serum albumin. Adv Protein Chem *45*, 153-203.

Castell, J.V., Gomez- Lechon, M.J., David, M., Fabra, R., Trullenque, R., and Heinrich, P.C. (1990). Acute- phase response of human hepatocytes: regulation of acute- phase protein synthesis by interleukin- 6. Hepatology *12*, 1179-1186.

Chen, B., Thurber, K.R., Shewmaker, F., Wickner, R.B., and Tycko, R. (2009). Measurement of amyloid fibril mass-per-length by tilted-beam transmission electron microscopy. Proc Nat Acad Sci USA *106*, 14339-14344.

Cohen, A.S., and Calkins, E. (1959). Electron microscopic observations on a fibrous component in amyloid of diverse origins. Nature *183*, 1202-1203.

Crippen, G.M., Rousaki, A., Revington, M., Zhang, Y.B., and Zuiderweg, E.R.P. (2010). SAGA: Rapid automatic mainchain NMR assignment for large proteins. J Biomol NMR *46*, 281-298.

Curry, S., Mandelkow, H., Brick, P., and Franks, N. (1998). Crystal structure of human serum albumin complexed with fatty acid reveals an asymmetric distribution of binding sites. Nat Struct Biol *5*, 827-835.

De Feo, P., Gaisano, M.G., and Haymond, M.W. (1991). Differential effects of insulin deficiency on albumin and fibrinogen synthesis in humans. J Clin Invest *88*, 866-840.

De Feo, P., Horber, F.F., and Haymond, M.W. (1992). Meal stimulation of albumin synthesis: a significant contributor to whole body protein synthesis in humans. Am J Physiol *263*, E799.

de la Arada, I., Seiler, C., and Mäntele, W. (2012). Amyloid fibril formation from human and bovine serum albumin followed by quasi-simultaneous Fourier-transform infrared (FT-IR) spectroscopy and static light scattering (SLS). Eur Biophys J *41*, 931-938.

Divry, P., and Florkin, M. (1927). Sur les proprietes optiques de l'amyloide. C R Soc Biol *97*, 1810.

Dockal, M., Carter, D.C., and Rüker, F. (2000). Conformational Transitions of the Three Recombinant Domains of Human Serum Albumin Depending on pH. J Biol Chem *275*, 3042-3050.

Dutta, S.K., Basu, S.K., and Sen, K.K. (2006). Binding of diclofenac sodium with bovine serum albumin at different temperatures, pH and ionic strengths. Indian J Exp Biol *44*, 123-127.

Eanes, E.D., and Glenner, G.G. (1968). X-ray diffraction studies on amyloid filaments. J Histochem Cytochem *16*, 673-677.

Edwards, R.A., and Woody, R.W. (1979). Spectroscopic studies of Cibacron Blue and Congo Red bound to dehydrogenases and kinases. Evaluation of dyes as probes of the dinucleotide fold. Biochemistry *18*, 5197-5204.

Elghetany, M.T., and Saleem, A. (1988). Methods for staining amyloid in tissues: a review. Stain Technol *63*, 201-212.

Fändrich, M., Fletcher, M.A., and Dobson, C.M. (2001). Amyloid fibrils from muscle myoglobin. Nature *410*, 165-166.

Feng, B.Y., Toyama, B.H., Wille, H., Colby, D.W., Collins, S.R., May, B.C.H., Prusiner, S.B., Weissman, J., and Shoichet, B.K. (2008). Small-molecule aggregates inhibit amyloid polymerization. Nat Chem Biol *4*, 197-199.

Ge, S., Kojio, K., Takahara, A., and Kajiyama, T. (1998). Bovine serum albumin adsorption onto immobilized organotrichlorosilane surface: influence of the phase separation on protein adsorption patterns. J Biomater Sci Polym Ed *9*, 131-150.

Geisow, M.J., and Beaven, G.H. (1977). Physical and binding properties of large fragments of human serum albumin. Biochem J *165*, 477-484.

Gosling, P. (1995). Albumin and the critically ill. Care Crit Lll *11*, 57-61.

Greenfield, N.J. (2006a). Analysis of the kinetics of folding of proteins and peptides using circular dichroism. Nat Protocol *1*, 2891-2899.

Greenfield, N.J. (2006b). Using circular dichroism collected as a function of temperature to determine the thermodynamics of protein unfolding and binding interactions. Nat Protoc *1*, 2527-2535.

Groenning, M. (2010). Binding mode of Thioflavin T and other molecular probes in the context of amyloid fibrils-current status. J Chem Biol *3*, 1-18.

Hardy., J., and Selkoe., D.J. (2002). The Amyloid Hypothesis of Alzheimer's Disease: Progress and Problems on the Road to Therapeutics. Science *297*, 353-356.

Harel, M., Sonoda, L.K., Silman, I., Sussman, J.L., and Rosenberry, T.L. (2008). Crystal structure of thioflavin T bound to the peripheral site of Torpedo californica acetylcholinesterase reveals how thioflavin T acts as a sensitive fluorescent reporter of ligand binding to the acylation site. J Am Chem Soc *130*, 7856-7861.

Holm, N.K., Jespersen, S.K., Thomassen, L.V., Wolff, T.Y., Sehgal, P., Thomsen, L.A., Christiansen, G., Andersen, C.B., Knudsen, A.D., and Otzen, D.E. (2007). Aggregation and fibrillation of bovine serum albumin. Biochim Biophys Acta *1774*, 1128-1138.

Hoye, R.C., Bennett, S.H., Geelhoed, G.W., and Gorschboth, C. (1972). Fluid volume and albumin kinetics occurring with major surgery. J Am Med Assoc *222,* 1261.

Hu, Y.J., Liu, Y., Shen, X.S., Fang, X.Y., and Qu, S.S. (2005). Studies on the interaction between 1-hexylcarbamoyl-5-fluorouracil and bovine serum albumin. J Mol Struct *738,* 143-147.

Hua, Y.J., Liua, Y., Zhanga, L.X., Zhaoa, R.M., and Qua, S.S. (2005). Studies of interaction between colchicine and bovine serum albumin by fluorescence quenching method. J Mol Struct *750,* 174-178.

Hutson, S.M., Stinson- Fisher, C., Shiman, R., and Jefferson, L.S. (1987). Regulation of albumin synthesis by hormones and amino acids in primary cultures of rat hepatocytes. Am J Physiol *250,* E291-E298.

Iadanza, M.G., Jackson, M.P., Radford, S.E., and Ranson, N.A. (2016). MpUL-Software for Calculation of Amyloid Fibril Mass per Unit Length from TB-TEM Images. Sci Rep *6,* 21078.

Jime´nez, J.L., Nettleton, E.J., Bouchard, M., Robinson, C.V., Dobson, C.M., and Saibil, H.R. (2002). The protofilament structure of insulin amyloid fibrils. Proc Natl Acad Sci USA *99,* 9196-9201.

Juárez, J., Taboada, P., and Mosquera, V. (2009). Existence of different structural intermediates on the fibrillation pathway of human serum albumin. Biophys J *96,* 2353-2370.

Kandagal, P.B., Ashoka, S., Seetharamappa, J., Shaikh, S.M., Jadegoud, Y., and Ijare, O.B. (2006). Study of the interaction of an anticancer drug with human and bovine serum albumin: spectroscopic approach. J Pharm Biomed Anal *41,* 393-399.

Kayed, R., Pensalfini, A., Margol, L., Sokolov, Y., Sarsoza, F., Head, E., Hall, J., and Glabe, C. (2009). Annular protofibrils are a structurally and functionally distinct type of amyloid oligomer. J Biol Chem *284,* 4230-4237.

Kayed, R., Head, E., Thompson, J.L., McIntire, T.M., Milton, S.C., Cotman, C.W., and Glabe, C.G. (2003). Common Structure of Soluble Amyloid Oligomers Implies Common Mechanism of Pathogenesis. Science *300,* 486-489.

Kendrew, J.C. (1954). Structure of proteins I. In The Proteins, Neurath, H., and Bailey, K. eds., (New York: Academic Press) pp. 893.

Khan, A.B., Khan, J.M., Ali, M.S., Khan, R.H., and Kabir-Ud-Din. (2012). Interaction of amphiphilic drugs with human and bovine serum albumins. Spectrochim Acta A Mol Biomol Spectrosc *97,* 119-124.

Khan, M.Y. (1986). Direct evidence for the involvement of domain III in the N-F transition of bovine serum albumin. Biochem J *236,* 307-310.

Khan, S.N., Islam, B., Yennamalli, R., Sultan, A., Subbarao, N., and Khan, A.U. (2008). Interaction of mitoxantrone with human serum albumin: spectroscopic and molecular modeling studies. Eur J Pharm Sci *35,* 371-382.

Khurana, R., Uversky, V.N., Nielsen, L., and Fink, A.L. (2001). Is Congo red an amyloid-specific dye? J Biol Chem *276,* 22715-22721.

Kim, Y.S., Randolph, T.W., Manning, M.C., Stevens, F.J., and Carpenter, J.F. (2003). Congo red populates partially unfolded states of an amyloidogenic protein to enhance aggregation and amyloid fibril formation. J Biol Chem *278,* 10842-10850.

Knaus, W.A., Wagner, D.P., Draper, E.A., Zimmerman, J.E., Bergner, M., Bastos, P.G., Sirio, C.A., Murphy, D.J., Lotring, T., and Damiano, A. (1991). The APACHE III prognostic system. Risk prediction of hospital mortality for critically ill hospitalized adults. Chest *100,* 1619-1636.

Krebs, M.R., Bromley, E.H., and Donald, A.M. (2005). The binding of thioflavin-T to amyloid fibrils: localisation and implications. J Struct Biol *149,* 30-37.

Lafaye, P., and Lapresle, C. (1988). Fixation of penicilloyl groups to albumin and appearance of anti-penicilloyl antibodies in penicillin-treated patients. J Clin Invest *82,* 7-12.

LeVine, H. (1995). Thioflavine T interaction with amyloid beta-sheets structures. Amyloid *2,* 1-6.

Lin, H., Lan, J., Guan, M., Sheng, F., and Zhang, H. (2009). Spectroscopic investigation of interaction between mangiferin and bovine serum albumin. Spectrochim Acta A Mol Biomol Spectrosc *73,* 936-941.

Lloyd, C.E., Kalinyak, J.E., Hutson, S.M., and Jefferson, L.S. (1987). Stimulation of albumin gene transcription by insulin in primary cultures of rat hepatocytes. Am J Physiol *252,* C205-C214.

Lundsgaard-Hansen, P. (1968). Physiology and pathophysiology of colloid osmotic pressure and albumin metabolism. Curr Stud Hematol Blood Transfus *53,* 1-17.

Majorek, K.A., Porebski, P.J., Dayal, A., Zimmerman, M.D., Jablonska, K., Stewart, A.J., Chruszcz, M., and Minor, W. (2012). Structural and immunologic characterization of bovine, horse, and rabbit serum albumins. Mol Immunol *52,* 174-182.

Maltsev, A.S., Grishaev, A., and Bax, A. (2012). Monomeric α-synuclein binds Congo Red micelles in a disordered manner. Biochemistry *51,* 631-642.

Militello, V., Vetri, V., and Leone, M. (2003). Conformational changes involved in thermal aggregation processes of bovine serum albumin. Biophys Chem *105,* 133-141.

Minghetti, P.P., Ruffner, D.E., Kuang, W.J., Dennison, O.E., Hawkins, J.W., Beattie, W.G., and Dugaiczyk, A. (1986). Molecular structure of the human albumin gene is revealed by nucleotide sequence within q11-22 of chromosome 4. J Biol Chem *261,* 6747-6757.

Moldave, K. (1985). Eukaryotic protein synthesis. Annu Rev Biochem *54,* 1109-1149.

Morisette, M., Weil, M.H., and Shubin, H. (1975). Reduction in colloid osmotic pressure associated with fatal progression of cardiopulmonary failure. Crit Care Med *3,* 115-117.

Moshage, H.J., Janssen, J., Franssen, J.H., Hafkenscheid, J.C.M., and Yap, S.H. (1987). Study of the molecular mechanism of decreased liver synthesis of albumin in inflammation. J Clin Invest *79,* 1635-1641.

Mouridsen, H.T. (1967). Turnover of human serum albumin before and after operations. Clin Sci *33*, 345-354.

Muchowski, P.J., Schaffar, G., Sittler, A., Wanker, E.E., Hayer-Hartl, M.K., and Hartl, F.U. (2000). Hsp70 and Hsp40 chaperones can inhibit self-assembly of polyglutamine proteins into amyloid-like fibrils. Proceedings of the National Academy of Sciences of the United States of America *97*, 7841-7846.

Naiki, H., Higuchi, K., Hosokawa, M., and Takeda, T. (1989). Fluorometric determination of amyloid fibrils in vitro using the fluorescent dye, thioflavin T1. Anal Biochem *177*, 244-249.

Oratz, M., Rothschild, M.A., and Schreiber, S.S. (1970). Effect of dextran infusions on protein synthesis by hepatic microsomes. Am J Physiol *218*, 1108-1112.

Pauling, L., and Corey, H.B. (1953). Two rippled sheet configurations of polypeptide chains, and a note about the pleated sheets. Proc Nat Acad Sci USA *39*, 253-256.

Perlmutter, D.H., Dinarello, C.A., Punsal, P.I., and Colten, H.R. (1986). Cachectin/tumor necrosis factor regulates hepatic acute-phase gene expression. J Clin Invest *78*, 1349-1354.

Peters, T. (1975). The Plasma Proteins: Structure Function and Genetic Control. Putman FW ed., (New York: Academic Press.) pp. 131-181.

Peters, T.J. (1996a). All About Albumin. Biochemistry, Genetics And Medical Applications. Academic Press ed., (San Diego: Academic Press) pp. 76-132.

Peters, T.J. (1996b). All About Albumin. Biochemistry, Genetics And Medical Applications. (San Diego: Academic Pres) pp. 188-250.

Peters, T.J. (1996c). All About Albumin. Biochemistry, Genetics And Medical Applications. (San Diego: Academic Press) pp. 1-8.

Peters, T.J. (1996d). All About Albumin. Biochemistry, Genetics And Medical Applications. Academic Press ed., (San Diego: Academic Press) pp. 188-250.

Peters, T.J. (1996e). Genetics: the albumin gene. In: All About Albumin. Biochemistry, Genetics, And Medical Applications. (San Diego: Academic Press) pp. 133-187.

Polymeropoulos, M.H., Lavedan, C., Leroy, E., Ide, S.E., Dehejia, A., Dutra, A., Pike, B., Root, H., Rubenstein, J., Boyer, R., *et al.* (1997). Mutation in the alpha-synuclein gene identified in families with Parkinson's disease. Science *276*, 2045−2047.

Puchtler, H., Sweat, F., and Levine, M. (1962). On the binding of congo red by amyloid. J. Histochem Cytochem *10*, 355-364.

Putnam, F.W. (1975). The Plasma Proteins: Structure, Function and Genetic Control. Putnam, Frank W. ed., (New York: Academic Press,) pp. 141.

Rasoulzadeh, F., Asgari, D., Naseri, A., and Rashidi, M.R. (2010). Spectroscopic studies on the interaction between erlotinib hydrochloride and bovine serum albumin. Daru *18*, 179-184.

Rombouts, I., Lagrain, B., Scherf, K.A., Koehler, P., and Delcour, J.A. (2015). Formation and reshuffling of disulfide bonds in bovine serum albumin demonstrated using tandem mass spectrometry with collision-induced and electron-transfer dissociation. Sci Rep *5*, 12210.

Rudyk, H., Vasiljevic, S., Hennion, R.M., Birkett, C.R., Hope, J., and Gilbert, I.H. (2000). Screening Congo Red and its analogues for their ability to prevent the formation of PrP-res in scrapie-infected cells. J Gen Virol *81*, 1151-1164.

Sakuma, K., Ohyama, T., Sogawa, K., Fujii-Kuriyama, Y., and Matsumura, Y. (1987). Low protein–high energy diet induces repressed transcription of albumin mRNA in rat liver. J Nutr *117*, 1141-1148.

Sawaya, M.R., Sambashivan, S., Nelson, R., Ivanova, M.I., Sievers, S.A., Apostol, M.I., Thompson, M.J., Balbirnie, M., Wiltzius, J.J., McFarlane, H.T., *et al.* (2007). Atomic structures of amyloid cross-beta spines reveal varied steric zippers. Nature *447*, 453-457.

Schröder, H., Langer, T., Hartl, F.U., and Bukau, B. (1993). DnaK, DnaJ and GrpE form a cellular chaperone machinery capable of repairing heat-induced protein damage. Embo J. *12*, 4137-44.

Sharma, R.N., and Pancholi, S.S. (2014). Protein binding interaction study of olmesartan medoxomil and its metabolite olmesartan by fluorescence spectroscopy. Int J Pharm Pharm Sci *6*, 726-729.

Shi, J.H., Wang, J., Zhu, Y.Y., and Chen, J. (2014). Characterization of intermolecular interaction between cyanidin-3-glucoside and bovine serum albumin: spectroscopic and molecular docking methods. Luminescence *29*, 522-530.

Shikama, Y., Kitazawa, J., Yagihashi, N., Uehara, O., Murata, Y., Yajima, N., Wada, R., and Yagihashi, S. (2010). Localized amyloidosis at the site of repeated insulin injection in a diabetic patient. Intern Med *49*, 397-401.

Shirahama, T., and Cohen, A.S. (1967). High-resolution electron microscopic analysis of the amyloid fibril. J Cell Biol *33*, 679-708.

Singleton, A.B., Farrer, M., Johnson, J., Singleton, A., Hague, S., Kachergus, J., Hulihan, M., Peuralinna, T., Dutra, A., Nussbaum, R., *et al.* (2003). alpha-Synuclein locus triplication causes Parkinson's disease. Science *302*, 841.

Sober, H.A. (1968). CRC Handbook of Biochemistry: Selected Data for Molecular Biology. Sober, H. A. ed., (Cleveland: The Chemical Rubber Company) pp. C-56.

Spillantini, M.G., Schmidt, M.L., Lee, V.M., Trojanowski, J.Q., Jakes, R., and Goedert, M. (1997). Alpha-Synuclein in Lewy bodies. Nature *388*, 839-840.

Sudlow, G., Birkett, D.J., and Wade, D.N. (1975). The characterisation of two specific drug binding sites on human serum albumin. Mol Pharmacol *11*, 824-832.

Sulatskaya, A.I., Maskevich, A.A., Kuznetsova, I.M., Uversky, V.N., and Turoverov, K.K. (2010). Fluorescence quantum yield of thioflavin T in rigid isotropic solution and incorporated into the amyloid fibrils. PLoS One *5*, e15385.

Tanwir, A., Jahan, R., Quadir, M.A., Kaisar, M.A., and Hossain, M.K. (2012). Spectroscopic Studies of the Interaction between Metformin Hydrochloride and Bovine Serum Albumin. Dhaka Univ J Pharm Sci *11,* 45-49.

Traylor, R.J., and Pearl, R.G. (1996). Crystalloid versus colloid versus colloid: all colloids are not created equal. Anesth Analg *83,* 209-212.

Uversky, V.N., and Permyakov, E.A. (2007). Methods in Protein Structure and Stability Analysis: Luminescence Spectroscopy and Circular Dichroism.

Vassar, P.S., and Culling, C.F. (1959). Fluorescent stains, with special reference to amyloid and connective tissues. Arch Pathol *68,* 487-498.

Walsh, D.M., and Selkoe, D.J. (2007). Ab Oligomers – a decade of discovery. Journal of Neurochemistry *101,* 1172-1184.

Wang, N., Ye, L., Zhao, B.Q., and Yu, J.X. (2008). Spectroscopic studies on the interaction of efonidipine with bovine serum albumin. Braz J Med Biol Res *41,* 589-595.

Weil, M.H., Henning, R.J., and Puri, V.K. (1979). Colloid oncotic pressure: clinical significance. Crit Care Med *7,* 113-116.

Westermark, G.T., Johnson, K.H., and Westermark, P. (1999). Staining methods for identification of amyloid in tissue. Methods Enzymol *309,* 3-25.

Wright, A.K., and Thompson, M.R. (1975). Hydrodynamic structure of bovine serum albumin determined by transient electric birefringence. Biophysical Journal *15,* 137-141.

Wu, C., Biancalana, M., Koide, S., and Shea, J.E. (2009). Binding modes of thioflavin-T to the single-layer beta-sheet of the peptide self-assembly mimics. J Mol Biol *394,* 627-633.

Wu, C., Wang, Z., Lei, H., Duan, Y., Bowers, M.T., and Shea, J.E. (2008). The binding of thioflavin T and its neutral analog BTA-1 to protofibrils of the Alzheimer's disease Abeta(16-22) peptide probed by molecular dynamics simulations.*384,* 718-729.

Yamauchi, A., Fukuhara, Y., Yamamoto, S., Yano, F., Takenaka, M., Imai, E., Noguchi, T., Tanaka, T., Kamada, T., and Ueda, N. (1992). Oncotic pressure regulates gene transcriptions of albumin and apolipoprotein B in cultured rat hepatoma cells. Am J Physiol *263,* C397-404.

Zhang, L., Liu, B., Li, Z., and Guo, Y. (2015). Comparative studies on the interaction of cefixime with bovine serum albumin by fluorescence quenching spectroscopy and synchronous fluorescence spectroscopy. Luminescence *30,* 686-692.

Appendix

Standard Operating Method - SDS-PAGE

I. Apparatus – Gel casting unit, Buffer tank with electrodes and power supply. [Biorad, Invitrogen] [1]

II. Reagents (see recipes in section VIII below)

1) pH 8.8, 1.5M Tris-HCl buffer (for separating gel)
2) pH 6.8, 0.5M Tris-HCl buffer (for stacking gel)
3) 30% Acrylamide Stock solution
4) TEMED solution (Tetramethylenediamine - sigma 6.63 M)
5) Solid anhydrous APS (Ammonium Persulfate - or 10% solution prepared fresh)
6) 10% SDS
7) pH 8.8 electrode running buffer

III. *Separating gel:*

1. Assemble the glass plate sandwich[1]. Prepare 5mL separating/resolving gel solution according to table below avoiding any bubble formation.
2. Pour the gel solution in glass sandwich leave about 1/4 of the space free for the stacking gel. Carefully cover the gel meniscus with DI water[3] and wait until the resolving gel polymerizes.
3. [A clear line will appear at the gel meniscus and water on top when polymerization is complete. TEMED+APS polymerizes solution so subsequent steps should be swift, adding too much TEMED/APS may cause quick polymerization in the beaker itself].

% gel	pH 8.8 buffer (mL)	Acryl. Stock (mL)	SDS 10% (mL)	DI H_2O (mL)	TEMED (µL)	APS[2]
20	1	3.3	.1	0.7	10	Few grains
18	1	3	.1	1	10	Few grains
16	1	2.7	.1	1.3	10	Few grains
15	1	2.5	.1	1.5	10	Few grains
14	1	2.3	.1	1.7	10	Few grains
12	1	2	.1	2	10	Few grains
11	1	1.83	.1	2.17	10	Few grains
10	1	1.67	.1	2.33	10	Few grains
9	1	1.5	.1	2.5	10	Few grains
8	1	1.33	.1	2.67	10	Few grains

IV. *Staking gel:* Prepare 2mL *stacking gel* according to Table II below (similar as section III). Wait for *separating gel* to polymerize, aspirate the water layer over it and add *stacking gel* on top and

immediately insert spacer to create sample loading wells [delay addition of TEMED/APS in *stacking gel* until you assure *separating gel* is polymerized].

% gel	pH 6.8 Buffer (mL)	Acryl Stock (mL)	SDS 10% (mL)	DI H_2O (mL)	TEMED (µL)	APS
4	0.5	0.27	.1	1.23	7	Few grains
5	0.5	0.33	.1	1.17	7	Few grains
6	0.5	0.40	.1	1.10	7	Few grains
7	0.5	0.47	.1	1.03	7	Few grains

V. Running gel:

1. Remove combs carefully, wash wells with water. Place the gel into the electrophoresis tank, fill the tank Running Buffer. Make sure there are no leaks and the wells are submerged in buffer.
2. Load markers and samples (mixed with loading buffer) boiled at 100 °C (optional) and run the gel at 200 mV (unless stated differently). Stop when the dye front reaches to bottom of the gel.

VI. Staining the Gel

Pry open the glass plates and free the sticky sides with a spatula. Invert it over a plastic container and let it fall under gravity. You may need to pull/push one end gently to set the fall. Pour Imperial (G250) or R250 commassie stain and microwave gel for 15 sec or leave the gel submerged in stain on shaker for 0.5 to 1 hr. Wash gel with water and then destain and leave it on shaker for desired time (few hrs to overnight). Take picture and document the results. *[Stain preparation - ……. Destain 50:40:10 Water:Methanol:Acetic acid]*

VII. Reagent Recipes:

pH 8.8 Buffer (1.5 M Tris-HCl)	pH 6.8 Buffer (0.5 M Tris-HCl)	30% Acrylamide Stock
→ Dissolve 181.71 g Tris base in 700 mL DI H_2O. Bring to pH 8.8 with concentrated HCl, bring volume to 1 L with additional H_2O (= 18.15g/100mL).	→ Dissolve 6 g Tris base in 60 mL DI H_2O. Adjust pH to 6.8 with concentrated HCl, then adjust volume to 100 mL with DI water.	→ Mix 29 g Acrylamide, 1 g Bisacrylamide, and bring volume to 100mL w/ DI H_2O (= 30%T; 3.3%C). Using 29.2 g Acryl. + 0.8 g Bisacryl. = 30%T, 2.6%C.

10% SDS (Sodium Dodecyl Sulfate)	Loading Dye (10 mL 6X Laemmli Buffer)	Electrode Running Buffer
Add 10 g SDS → 80 mL DI H_2O. Allow to dissolve, then bring to 100mL w/ additional H_2O.	Dissolve 6 mg Bromophenol Blue in 2.1 mL DI H_2O, then add the following: 1) 1.2 g SDS	Add the following to 1.8 L DI H_2O: - 28.8 g glycine (14.4g/500mL)

	2) 1.2 mL pH 6.8 Tris buffer 3) 4.7 mL glycerol → Warm and dissolve everything.	- 6.04 g Tris base (3.02g/500mL) - 2 g SDS (5g/500mL) → Once dissolved, add H_2O till volume = 2 L, pH will be 8.8 no need to check.

[1] See the SOM for PAGE Apparatus and Assembly
[2] Best way to control APS addition is by adding from a solution (10%) freshly prepared or frozen (-20C) [10-25µL]
[3] The separating/resolving gel can be covered with 50% isopropanol, 0.1% SDS solution or water

Expected %age gel for running expected molecular wt range:
66kDa (~9%) 10kDa (≥15%)
[A gradient gel with concentration uniformly varying from 4% at the top to 20% at bottom is universal for running any protein independent of its size]

Notes:

- SDS-PAGE [Sodium Dodecyl Sulfate PolyAcrylamide Gel Electrophoreses] is a technique used in biochemistry to separate molecules based on their size. By adjusting the total amount of acrylamide (%T) and cross-linking bisacrylamide (%C), you can make a gel with different pore sizes. This will govern the distance which a given protein will be able to travel under an electrical current.
- Addition of the DI water layer on top of the separating gel prevents its top from drying. This will ensure current will travel between the stacking and separating layers' junction once it has polymerized. Isopropanol was traditionally used for this purpose.
- Running gels of lower percentage (than listed) runs the risk of the gel falling apart at the touch, or stretching like plastic, ruining the results.
- Besides %T pore size can be adjusted with the cross-linker (%C).